

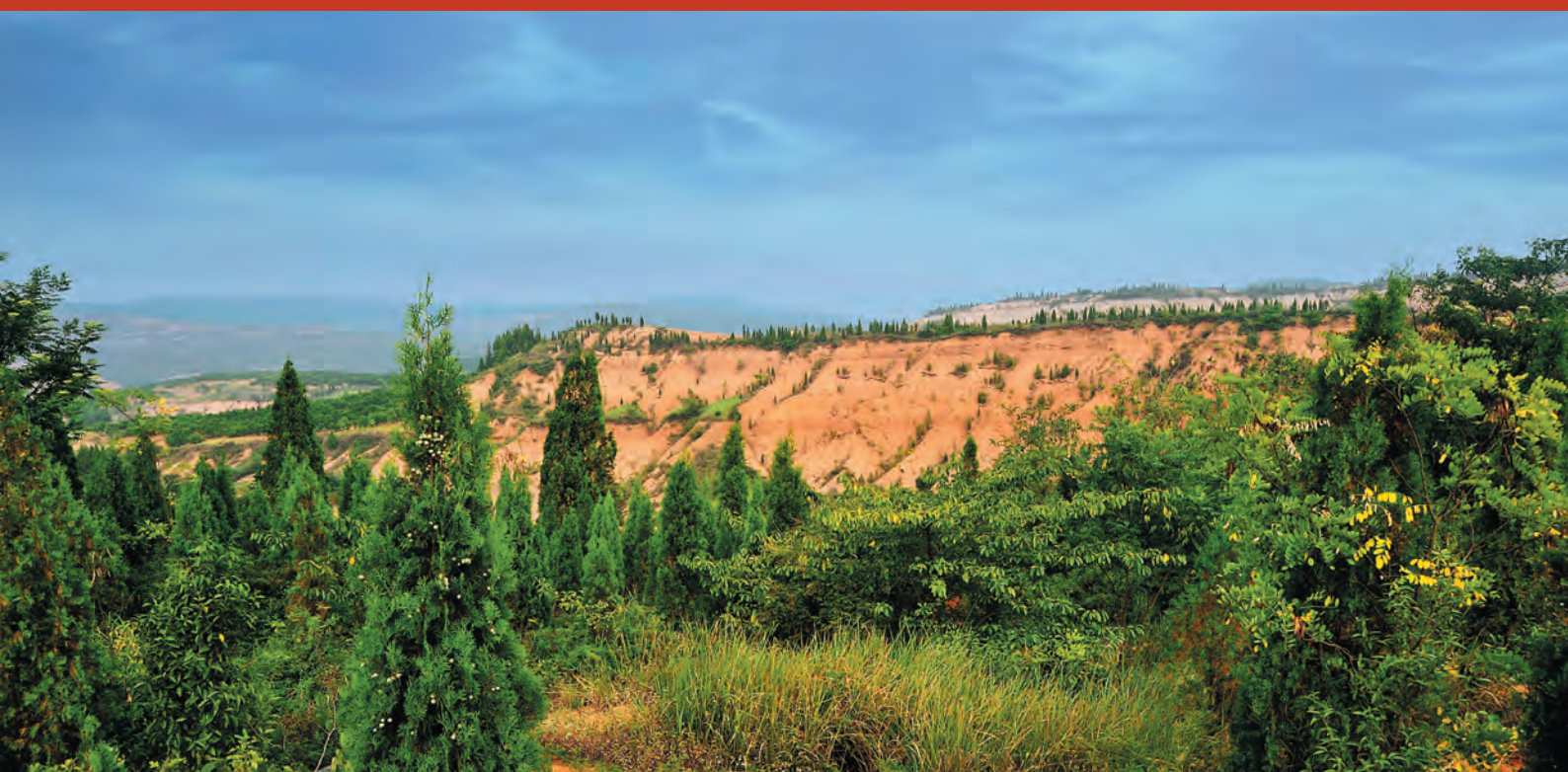
Global changes of net primary productivity, affected by climate and abrupt land use changes since 1981

Towards mapping global soil degradation



World Soil Information

ISRIC Report 2013/01



J.G. Conijn, Z.G. Bai, P.S. Bindraban and B. Rutgers



Global changes of net primary productivity, affected by climate and abrupt land use changes since 1981

Towards mapping global soil degradation

J.G. Conijn¹, Z.G. Bai², P.S. Bindraban^{1,2} and B. Rutgers²

¹ Plant Research International, Wageningen, the Netherlands

² ISRIC – World Soil Information, P.O. Box 353, 6700 AJ, Wageningen, the Netherlands

ISRIC Report 2013/01

Wageningen, April 2013



© 2013, ISRIC – World Soil Information, Wageningen, Netherlands

All rights reserved. Reproduction and dissemination for educational or non-commercial purposes are permitted without any prior written permission provided the source is fully acknowledged. Reproduction of materials for resale or other commercial purposes is prohibited without prior written permission from ISRIC. Applications for such permission should be addressed to:

Director, ISRIC – World Soil Information

PO BOX 353

6700 AJ Wageningen

The Netherlands

E-mail: soil.isric@wur.nl

The designations employed and the presentation of materials do not imply the expression of any opinion whatsoever on the part of ISRIC concerning the legal status of any country, territory, city or area or of its authorities, or concerning the delimitation of its frontiers or boundaries.

Despite the fact that this publication is created with utmost care, the authors(s) and/or publisher(s) and/or ISRIC cannot be held liable for any damage caused by the use of this publication or any content therein in whatever form, whether or not caused by possible errors or faults nor for any consequences thereof.

Additional information on ISRIC – World Soil Information can be accessed through <http://www.isric.org>

Citation

Conijn, J.G., Z.G. Bai, P.S. Bindraban, B. Rutgers 2013. *Global changes of net primary productivity, affected by climate and abrupt land use changes since 1981. Towards mapping global soil degradation*. Report 2013/01, ISRIC – World Soil Information, Wageningen.



ISRIC Report 2013/01

Contents

List of acronyms and abbreviations	7
1 Introduction	9
2 Description of data sets	11
2.1 Σ NDVI	11
2.2 TBW	12
2.3 NPP	13
2.4 Final data sets	14
3 Regression results	15
3.1 Σ NDVI as function of TBW	15
3.2 NPP as function of Σ NDVI or TBW	15
4 NPP change maps	19
5 Model sensitivity analysis	21
5.1 Standard run of Miscanthus	21
5.2 Irrigated run of Miscanthus	24
5.3 Run with red=0.5 for Miscanthus	24
5.4 Reed canary grass	25
6 Detecting abrupt changes in NDVI	29
6.1 NDVI variations in areas with/without LUC in the Argentinean Chaco region	29
6.2 NDVI variations in the areas with/without LUC in the Argentinean Salta province	34
6.3 NDVI variations in burnt and non-burnt areas in the Southeastern Russia	36
6.4 NDVI variations in areas with/without deforestation in the DR of the Congo	41
7 Discussion and conclusions	47
Acknowledgements	51
References	53
Appendix I Global mapping of abrupt changes	57

List of figures

Figure 1	Degree of confidence of changes in Σ NDVI 1981–2006. Negative refers to an overall decline in Σ NDVI over the period and positive to an overall increase.	11
Figure 2	Degree of confidence of changes in TBW 1981–2006. Negative refers to an overall decline in TBW over the period and positive to an overall increase.	13
Figure 3	Scatter plot of the relation between mean values of Σ NDVI and NPP (2000–2006; only 1% of all data are shown, which have been randomly selected), including the regression line $NPP = 24.6 + 37.9*\Sigma NDVI + 9.09*(\Sigma NDVI)^2$ (based on the entire dataset).	16
Figure 4	Scatter plot of the relation between mean values of TBW and NPP (2000–2006; only 1% of all data are shown, which have been randomly selected), including the regression line $NPP = 106 + 18.8*TBW - 0.0884*(TBW)^2$ (based on the entire dataset).	16
Figure 5	Actual change of estimated mean NPP (expressed as percentage per year) for the period 1981–2006.	19
Figure 6	Climate-induced change of estimated mean NPP (expressed as percentage per year) for the period 1981–2006.	20
Figure 7	Non-climate related part of actual change of estimated mean NPP (expressed as percentage per year) for the period 1981–2006.	20
Figure 8	Cumulative frequency distribution of (a) TBW and (b) c%TBW of the standard run of Miscanthus for all unique climate-soil combinations with average TBW > 0 (n = 404,085).	21
Figure 9	Cumulative frequency distribution of the t-value of the slope of the standard run of Miscanthus for all unique climate-soil combinations with average TBW > 0 and standard deviation of slope > 0 (n = 404,067).	22
Figure 10	Relation between (a - left) c%TBW and TBW and (b - right) c%TBW and number of suitable years within the period 1981–2006 for the standard run of Miscanthus (average TBW > 0; n = 404,085).	22
Figure 11	Relation between (a) average TBW and cumulative precipitation in the growth period (PreGP) and between (b) c%TBW and c%PreGP during 1981–2006 of the standard run of Miscanthus (average TBW > 0; n = 404,085).	23
Figure 12	Relation between (a – left) TBW and (b – right) c%TBW of the irrigated run and the standard (= non-irrigated) run of Miscanthus (average TBW > 0; n = 404,085).	24
Figure 13	Relation between (a – left) TBW and (b – right) c%TBW of the run with red=0.5 and the standard run of Miscanthus (average TBW > 0; n = 404,085).	25
Figure 14	Cumulative frequency distribution of (a – left) TBW and (b) c%TBW (b – right) of the run of Reed Canary grass for all unique climate-soil combinations with average TBW > 0 (n = 396,393).	25
Figure 15	Cumulative frequency distribution of the t-value of the slope of the run of Reed Canary grass for all unique climate-soil combinations with average TBW > 0 (n = 396,393).	25
Figure 16	Land use change (left, data from Adámoli <i>et al.</i> , 2011, 1-5 are the selected sites) and abrupt trend change in NDVI (right, data from de Jong <i>et al.</i> , 2012) in the Chaco region.	30
Figure 17	Σ NDVI variations 1981–2006 with/without LUC in the Chaco region, Argentina (five sites, based on the LUC map made by Adámoli <i>et al.</i> , 2011).	31
Figure 18	Difference between multi-year mean Σ NDVI and minimum Σ NDVI for the Chaco region (left, ≥ 1.454) and for the areas with changes in land use (right, average value ≥ 1.185).	33
Figure 19	Percentage of $(\Sigma NDVI_{avg} - \Sigma NDVI_{min})/\Sigma NDVI_{avg}$ larger than 20% (left), standard deviation of annual Σ NDVI (right) in the Chaco region, Argentina.	34
Figure 20	Land use change during 1981–2006 (left, 1–5 are the selected sites) and abrupt trend in NDVI (right) in Salta province, Argentina.	35
Figure 21	NDVI variations 1981–2006 at sites with/without LUC indicated in the headings of each graphs in the Salta province, Argentina.	36
Figure 22	Wildfire in SE Russia from 1996 to 2002.	37
Figure 23	Top: aggregation of areas affected by wildfire events for the period of 1996–2002; sites 1–6 are the selected sites; bottom: abrupt trend change in NDVI over 1982–2008 (de Jong <i>et al.</i> , 2012).	38
Figure 24	Σ NDVI variations in the burnt and no burnt areas in SE Russia.	39

Figure 25	Forest cover and loss within 2000–2005 and 2005–2010 in the DR of the Congo.	42
Figure 26	Forest cover loss within 2000–2005 in a part of the DR of the Congo, 1–5 are the selected sites.	43
Figure 27	NDVI variations in the areas with/without forest loss in the DR of the Congo.	44
Figure A1	Differences between multi-year mean Σ NDVI and minimum Σ NDVI during 1981–2006	57
Figure A2	Percentage of $(\text{Mean } \Sigma\text{NDVI} - \text{Min } \Sigma\text{NDVI}) / \text{Mean } \Sigma\text{NDVI}$ from 1981–2006.	57
Figure A3	Standard deviation of annual Σ NDVI from 1981–2006.	58

List of tables

Table 1	Cumulative percentage of the number of years with/without growth within 1981–2006 for the standard run of <i>Miscanthus</i> and average TBW > 0 (maximum number = 26).	23
Table 2	Some data on mean TBW and mean c%TBW.	26
Table 3	Cumulative percentage of the number of years with growth within 1981–2006 for the run with Reed canary grass and average TBW > 0 (maximum number = 26).	26
Table 4	Statistics of NDVI, land cover and LUC at five sites in the Chaco region, Argentina.	32
Table 5	Statistics of NDVI, land cover and LUC of four sites in the Salta province, Argentina.	35
Table 6	Statistics of NDVI in the burnt and non-burnt areas in Southeast Russia.	40
Table 7	Statistics of NDVI in the areas with/without forest loss in the DR of the Congo.	45

List of acronyms and abbreviations

AVHRR	Advanced Very High Resolution Radiometer
CRU	Climate Research Unit, University of East Anglia
EMD	Empirical Mode Decomposition
ESA	European Space Agency
FAO	Food and Agriculture Organization of the United Nations, Rome
F_{PAR}	Fraction of absorbed Photosynthetically Active Radiation
GIMMS	Global Inventory Modelling and Mapping Studies, University of Maryland
GMAO	The Global Modeling and Assimilation Office
HANTS	Harmonic Analyses of NDVI Time-Series
IMAGE-GLOBIO	Integrated Model to Assess the Global Environment - Global Biodiversity Model
ISRIC	International Soil Reference Information Centre
JRC	European Commission Joint Research Centre
LAI	Leaf Area Index
Landsat ETM+	Land Resources Satellite, Enhanced Thematic Mapper
LINPAC	A LINtul model for Perennial and Annual Crops
LUS	Land Use Systems, FAO
MOD17A3	MODIS 8-Day Net Primary Productivity data set
MODIS	Moderate-Resolution Imaging Spectroradiometer
MVC	Maximum Value Composite
NDVI	Normalized Difference Vegetation Index
NOAA	The US National Oceanic and Atmospheric Administration
NPP	Net Primary Productivity
PBL	Netherlands Environmental Assessment Agency
SZA	Solar Zenith Angle
TBW	Total annual production of biomass
WISE	A harmonized Dataset of Derived Soil Properties for the World

1 Introduction

In a previous study (Bai *et al.*, 2012), global changes of remotely sensed greenness (NDVI) and simulated biomass production (TBW) since 1981 have been analysed for the purpose of mapping global soil degradation. The objective of the current research is to refine the findings of this previous research, to more clearly identify areas (grid cells) affected by land degradation. As a start further fine-tuning is needed to improve (non-)linear correlations between various parameters in the analysis. Next, the aggregate impact of climate and the impact of human interventions causing abrupt changes like de- or reforestation should be quantified in a global context. This information can be used to correct the changes in greenness observed via NDVI and better identify areas that were exposed to land degradation and/or improvement. Other factors that cause land degradation and/or improvement fall outside the scope of this study and the results are therefore first steps in mapping land degradation. New maps will be created by linking the (corrected) changes in greenness to Net Primary Productivity (NPP) and these can be used for further analysis in other projects. The results from this report are used as input for the PBL project 'Biodiversity, Ecosystem services and Development' to assess the effects of land degradation on future economic development and biodiversity around the world (using the global model IMAGE). Moreover, results will also be verified in a related project by comparing changes in NDVI, TBW and NPP with local expert judgment from selected countries/areas.

2 Description of data sets

2.1 Σ NDVI

The Normalized Difference Vegetation Index (NDVI) is calculated from the red (RED) and near-infrared (NIR) light reflected by the Earth's surface, *i.e.*, $NDVI = (NIR-RED)/(NIR+RED)$, and is used as a measure of vegetation or greenness. The NDVI data used in this study are produced by the Global Inventory Modelling and Mapping Studies (GIMMS) group from measurements made by the AVHRR radiometer on board of the US National Oceanic and Atmospheric Administration satellites (US-NOAA) (Tucker *et al.*, 2004; Pinzon *et al.*, 2007). The fortnightly images at 8km-spatial resolution, derived from daily 4 km global area coverage, are corrected for view geometry, volcanic aerosols, and other effects not related to vegetation cover (Tucker *et al.*, 2005). The maximum-value-composite (MVC) technique is used to remove bias caused by atmospheric conditions (Holben, 1986). Orbital drift correction is performed using an empirical mode decomposition (EMD) transformation method of Pinzon *et al.* (2005) removing common trends between time series of solar zenith angle (SZA) and NDVI. Orbital decay and changes in NOAA satellites affect AVHRR data but processed NDVI data have been found to be free of trends introduced from these effects (Kaufmann *et al.*, 2000). No atmospheric correction is applied to the GIMMS data except for volcanic stratospheric aerosol periods (1982–1984 and 1991–1994) (Tucker *et al.*, 2005); some uncertainty still remains, especially in hazy and cloudy conditions (Nagol *et al.*, 2009).

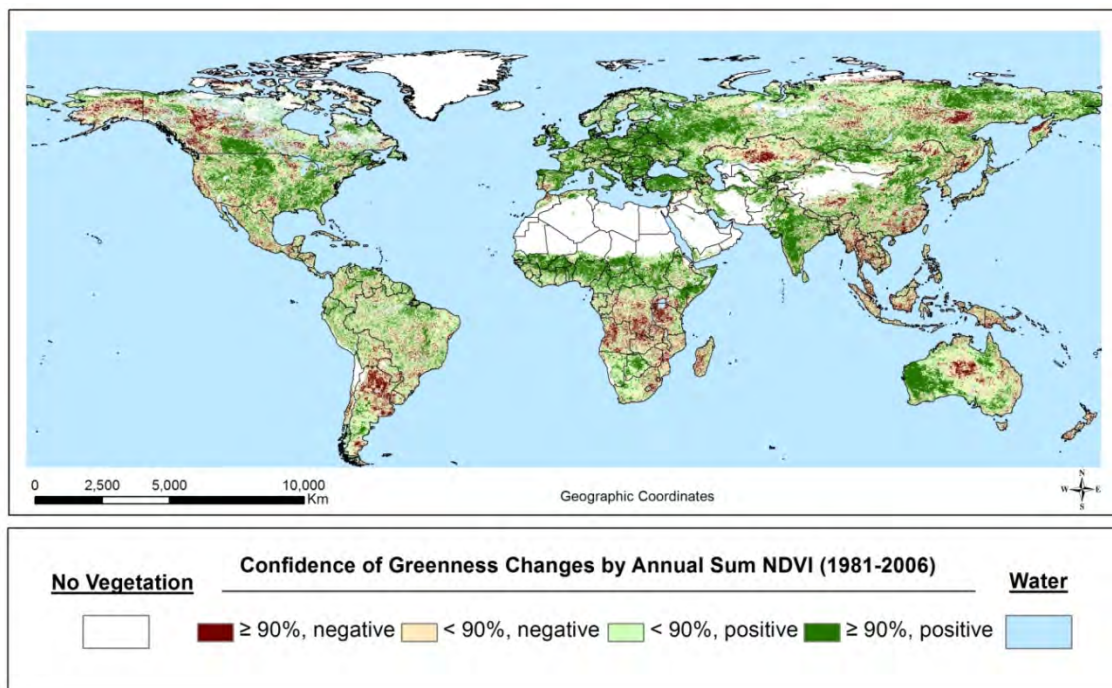


Figure 1

Degree of confidence of changes in Σ NDVI 1981–2006. Negative refers to an overall decline in Σ NDVI over the period and positive to an overall increase.

To remove any residual cloud effects or other outliers, the Harmonic Analysis of NDVI Time-Series (HANTS) algorithm (Verhoef *et al.*, 1996; Roerink *et al.*, 2000; Wit & Su, 2005) has been applied to smoothen and reconstruct the NDVI time-series (de Jong *et al.*, 2012); the HANTS-reconstructed data from July 1981 to December 2006 was employed and annual sum NDVI or Σ NDVI is used as a proxy for annual greenness in this study. Simple linear trend analysis has been performed to indicate changes in Σ NDVI over time (1981–2006). Figure 1 shows two levels of significance for the Σ NDVI trend analysis by Bai and colleagues (2012).

2.2 TBW

Total annual production of biomass (TBW) was calculated for every year in the period 1981–2006 with the crop model LINPAC (Conijn *et al.*, 2011; Jing *et al.*, 2012) and refers to the rain-fed production level, *i.e.* optimum management but not irrigated, ample nutrient availability and free from pests, diseases and weeds. The model has a time step of one day and calculates daily biomass increase based on crop characteristics, soil and weather data: including soil texture, soil depth, soil water holding capacity, radiation, temperature, precipitation, vapour pressure and wind speed. Daily soil water availability and (evapo)transpiration following from a soil water balance calculation, and daily leaf area growth are intermediate variables. Accumulation of daily biomass production over the season leads to total biomass production and yield. Prior to the biomass calculation, the suitability of each grid cell for cropping under rain-fed conditions is checked per year as function of temperature, soil water availability and crop characteristics leading to calculated sowing and harvesting dates of all crop cycles in a year. For annual crops the number of cycles per year ranges from 0 to an assumed maximum of three and is found by ‘fitting’ temperature sum requirements of a crop into the period of suitable growing days per year (see also Conijn *et al.*, 2011a). For perennial vegetation the plant growth period equals the period of suitable growing conditions. For this study two runs were separately executed to calculate the biomass production of an annual and a perennial vegetation and TBW has been found by combining the results of the two runs on the basis of the crop land fraction (f_{crop}) in each grid cell:

$$\text{TBW} = f_{\text{crop}} * \text{TBW}_{\text{annual}} + (1 - f_{\text{crop}}) * \text{TBW}_{\text{perennial}}$$

If one of the two model runs (annual or perennial) produces a zero value in a grid cell, the TBW of this cell is estimated by the value of the other run:

$$\begin{aligned} \text{TBW} &= \text{TBW}_{\text{perennial}} && \text{if } \text{TBW}_{\text{annual}} = 0 \\ \text{TBW} &= \text{TBW}_{\text{annual}} && \text{if } \text{TBW}_{\text{perennial}} = 0 \end{aligned}$$

Time series of gridded weather data (monthly averages/totals) from the Climate Research Unit (CRU, 2011) were used as input with a resolution of 30x30 arc-minutes. Daily values are calculated by a random distribution function for precipitation and by linear interpolation for the other climate variables. Soil characteristics were obtained from the ISRIC-WISE v1.0 database (Batjes, 2006) in combination with the Digital Soil Map of the World from FAO with a resolution of 5x5 arc-minutes (FAO, 1996). The land use map of Erb *et al.* (2007) was used to estimate the crop land fraction with a resolution of 5x5 arc-minutes. The annual crop has been approximated by taking the characteristics of a wheat/maize crop as input (wheat for temperate and maize for tropical regions) and those of Miscanthus to represent the perennial vegetation. Some parameters were adapted to ensure that in locations with short growing seasons (*e.g.* in dry or cold climates) vegetation types with shorter growth cycles compared to wheat, maize or Miscanthus could also be simulated.

Because soil and crop characteristics are kept constant, the calculated biomass production will reflect the impact of changes in climate over time.

Simple linear trend analysis is used to indicate changes in TBW over time (1981–2006). Figure 2 shows two levels of significance for the TBW trend analysis (from Bai *et al.*, 2012).

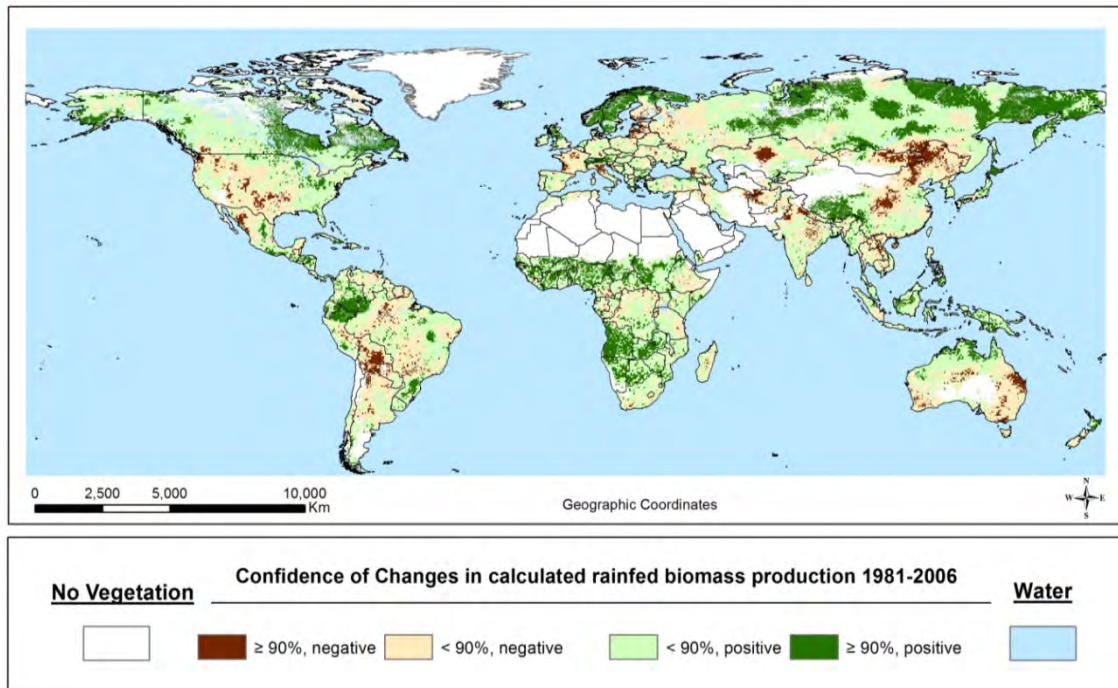


Figure 2

Degree of confidence of changes in TBW 1981–2006. Negative refers to an overall decline in TBW over the period and positive to an overall increase.

2.3 NPP

MODIS (Moderate-Resolution Imaging Spectro-Radiometer) MOD17A3 is a dataset of terrestrial gross and net primary productivity, computed at 1-km resolution at an 8-day interval with daily MODIS land cover, F_{PAR}/LAI and global GMAO (Global Modeling and Assimilation Office) surface meteorology at 1km for the global vegetated land surface (Heinsch *et al.*, 2003; Running *et al.*, 2004; Zhao *et al.*, 2005; Zhao & Running, 2010). The dataset produces daily gross primary production and sums to net primary production at the end of the year. The NPP data have been validated in various landscapes (Fensholt *et al.*, 2004; 2006; Gebremichael & Barros, 2006; Turner *et al.*, 2003; 2006) indicating that the calculated NPP are reliable at the regional scale (Zhao *et al.*, 2005; 2006). The MOD17A3 is continuously produced and available till 2011; the improved MOD17A3 from 2000 through to 2006 which matches the available HANTS-reconstructed NDVI dataset, is used in this study to indicate non-vegetated areas for which NPP is assumed zero and to correlate with $\Sigma NDVI$ and TBW.

2.4 Final data sets

The data of NPP and Σ NDVI that originally had a higher resolution were rescaled to the lower resolution of TBW (5x5 arc-minutes) to allow correlations between NPP, Σ NDVI and TBW. For all three data annual values are available from 2000–2006 (NPP) and 1981–2006 (Σ NDVI and TBW). The annual values have been used to calculate (a) mean values per grid cell, averaged over 2000–2006 (NPP, Σ NDVI and TBW) and 1981–2006 (Σ NDVI and TBW) and (b) average changes over 1981–2006 per grid cell by linear regression against time (Σ NDVI and TBW; Bai *et al.* 2012). The mean values per grid cell were used for correlations and together with the average changes of Σ NDVI and TBW also for estimating changes in mean NPP. For determining the correlation between mean NPP or Σ NDVI and TBW all grid cells where TBW cannot be calculated, e.g. due to missing weather data, have been excluded. For the correlation between mean NPP and Σ NDVI or TBW and the related calculation of the NPP change maps, all grid cells with mean NPP = 0 (2000–2006), according to the MODIS data set, have been excluded prior to the calculation of the regression and changes in NPP. This was done in order to limit the research to vegetated areas with mean NPP > 0 (according to MODIS for the period 2000–2006). Non-relevant changes, where the absolute relative value (% change) is lower than a threshold, were not excluded before-hand, but a threshold has been used to highlight those cells in the maps of NPP change. For this a threshold of 0.2% per year has been applied (equivalent to 5% over 26 years). Statistical non-significant changes (Figures 1 & 2) were also not excluded before-hand. This information can be used as an additional layer to the NPP change maps to highlight the statistical significance of changes over time in Σ NDVI and TBW on which the NPP change maps are based.

3 Regression results

3.1 Σ NDVI as function of TBW

To investigate a possible improvement in the relation between Σ NDVI as function of TBW (as published in Bai *et al.* 2012), one global equation was compared with a set of several equations to capture land cover variability in land cover with all equations having the form of Σ NDVI = $a + b * \sqrt{TBW}$. Spatial land cover data from Erb *et al.* (2007) were used to create four subsets, differing in dominant land cover, from the global original data set. One global equation using all data (n = 1,867,010) has an adjusted R² of 0.655 and the four equations separated by land cover have respectively

adjusted R ² = 0.587	(cells with fraction grassland >= 0.67;	n = 473,088),
adjusted R ² = 0.311	(cells with fraction crop land >= 0.67;	n = 67,274),
adjusted R ² = 0.544	(cells with fraction forest >= 0.67;	n = 392,085),
adjusted R ² = 0.641	(all remaining cells;	n = 934,563).

The combination of the four equations (n = 1,867,010) has an adjusted R² of 0.674. It can be concluded that the four equations combined only give a small improvement of the total adjusted R² by +0.02. Hence, distinguishing land cover type will not improve the analysis.

Another (multiple) linear regression analysis has been performed with one global equation, but including the different land covers of each grid cell continuously:

$$\Sigma NDVI = a + b * \sqrt{TBW} + c * \%grass + d * \%crop + e * \%forest$$

This equation has an adjusted R² of 0.705, indicating an increase of 0.05 compared to the simple linear regression above. Although this improvement may seem relevant, the use of land cover data in the relation between Σ NDVI and TBW is not used further in this study because the change in land cover over time during 1981–2006 is not known, contrary to the changes in Σ NDVI and TBW. Changes in NPP cannot be explained adequately with equation(s) containing land cover data if the changes in land cover in each grid cell are unknown.

3.2 NPP as function of Σ NDVI or TBW

For calculating changes in NPP as function of Σ NDVI and TBW, a more direct approach was used by correlating NPP to Σ NDVI and NPP to TBW using mean values per pixel based on the annual values averaged over 2000–2006. Both relations obtained for this period are based on the spatial variation over all grid cells and they are also assumed valid for the period 1981–2006. Moreover, it is assumed that these relations can be used to estimate the NPP changes over time of each grid cell based on the temporal changes of Σ NDVI and TBW per grid cell. The relation between NPP and Σ NDVI is used to estimate the change in NPP as function of Σ NDVI change during 1986–2006, assuming that a change in NPP (productivity) is reflected by a change in Σ NDVI (greenness), irrespective of the cause of these changes. The relation between NPP and TBW and the changes in TBW are used for estimating the climate-induced NPP change, because changes in calculated TBW are only caused by differences in the climatic variables during 1981–2006 that are used in the simulation.

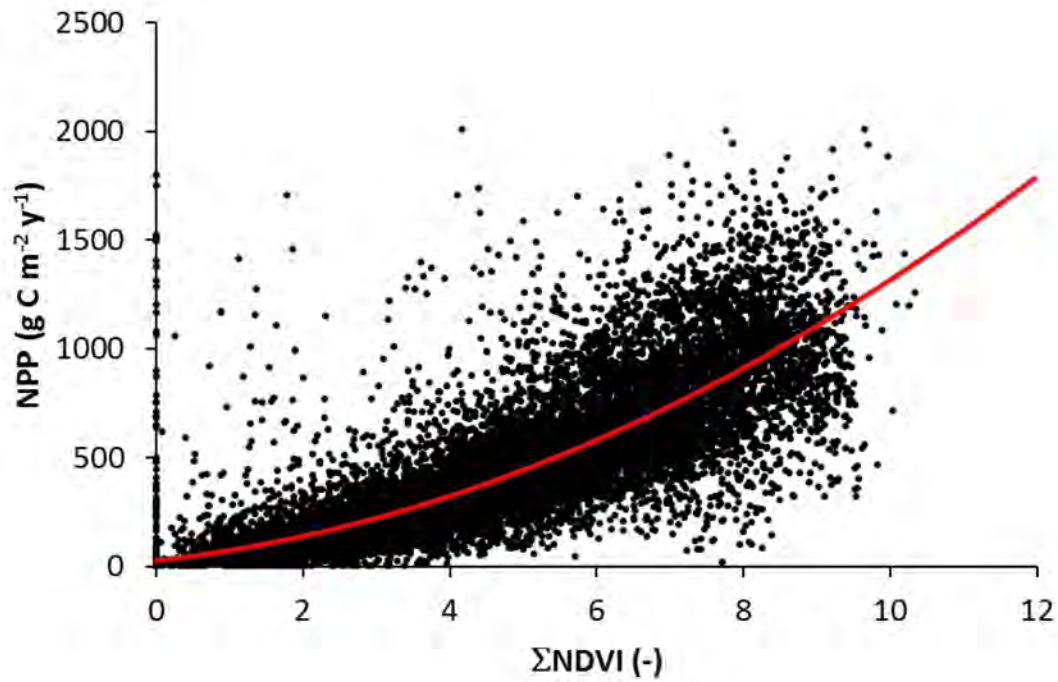


Figure 3
 Scatter plot of the relation between mean values of ΣNDVI and NPP (2000–2006; only 1% of all data are shown, which have been randomly selected), including the regression line $\text{NPP} = 24.6 + 37.9 \cdot \Sigma\text{NDVI} + 9.09 \cdot (\Sigma\text{NDVI})^2$ (based on the entire dataset).

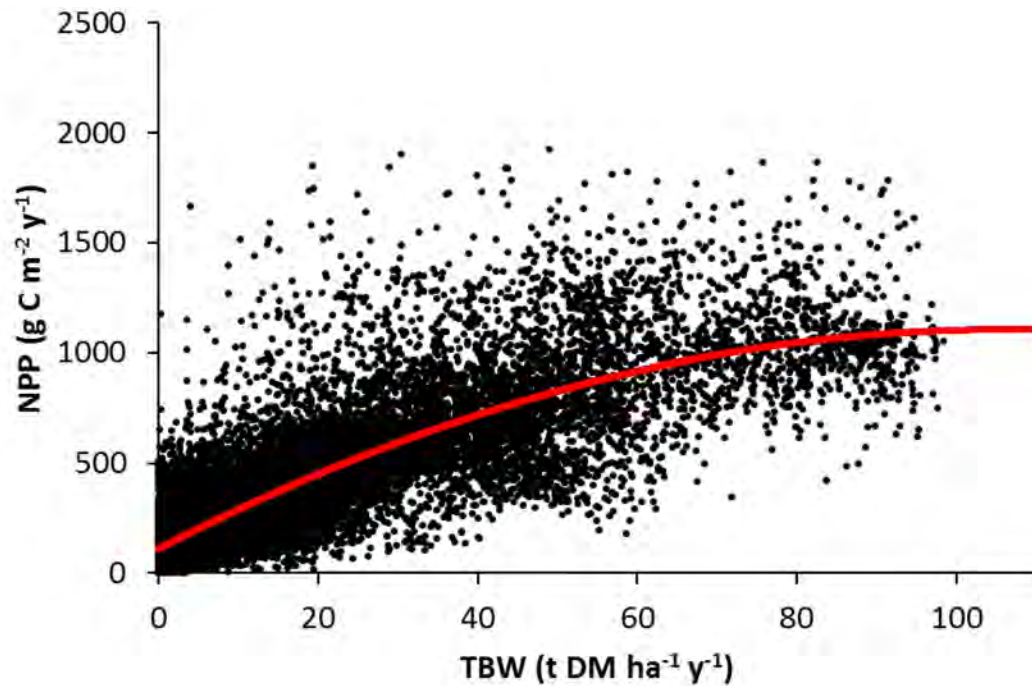


Figure 4
 Scatter plot of the relation between mean values of TBW and NPP (2000–2006; only 1% of all data are shown, which have been randomly selected), including the regression line $\text{NPP} = 106 + 18.8 \cdot \text{TBW} - 0.0884 \cdot (\text{TBW})^2$ (based on the entire dataset).

The remaining change in NPP, *i.e.* the difference between total NPP change as function of Σ NDVI and climate-induced NPP change as function of TBW, is then caused by non-climatic factors. Several different equations were tested to identify the best relation between the response variable NPP and the explanatory variables Σ NDVI and TBW, including linear, quadratic, logistic, exponential, hyperbolic, Richards and Gompertz. A quadratic equation was selected for both relations, because it performed better (compared to the linear equation) or similar (compared to the other curve-linear equations) with respect to the adjusted R^2 .

For NPP, Σ NDVI and TBW as mean values per grid cell during 2000–2006 the following global equations were fitted:

$$NPP = a + b * \Sigma NDVI + c * (\Sigma NDVI)^2 \quad (n=1,909,813; \text{adjusted } R^2 = 0.693) \quad (1)$$

$$NPP = d + e * TBW + f * (TBW)^2 \quad (n=1,751,128; \text{adjusted } R^2 = 0.663) \quad (2)$$

4 NPP change maps

Changes in NPP during 1981–2006 were estimated by using equations 3 – 5 where parameters b – f refer to eqn. 1 and 2 and $\Sigma\text{NDVI}_{\text{trend}}$ and $\text{TBW}_{\text{slope}}$ represent the average changes over time based on linear regressions of annual values from 1981–2006 on time, as already reported by Bai and colleagues (2012). tNPP refers to the actual change in NPP as estimated from changes in ΣNDVI , cNPP is the change in NPP expected from the change in climate (estimated by the change in TBW) and nNPP is an estimate for the non-climate related part of the actual NPP change and refers to changes such as in land cover/use, crop management and soil degradation. The first part of equation 3 (between brackets) equals the derivative of equation 1 ($d\text{NPP}/d\Sigma\text{NDVI}$) and the second part represents the derivative of the function relating ΣNDVI to time ($d\Sigma\text{NDVI}/dt$). By multiplying both parts the change of mean NPP over time is calculated ($d\text{NPP}/dt$). The same holds for equation 4 and 2 with respect to NPP and TBW, where the climate-induced NPP change is estimated.

$$\text{tNPP} = (b + 2 * c * \Sigma\text{NDVI}) * \Sigma\text{NDVI}_{\text{trend}} \quad (3)$$

$$\text{cNPP} = (e + 2 * f * \text{TBW}) * \text{TBW}_{\text{slope}} \quad (4)$$

$$\text{nNPP} = \text{tNPP} - \text{cNPP} \quad (5)$$

Furthermore mean NPP values for 1981–2006 (NPP_e) were estimated by using equation 1 in combination with mean values for ΣNDVI of the period 1981–2006 (note: the MODIS database used in this study only contained data from 2000–2006 of which mean NPP values were used for estimating the parameters of eqn. 1 and 2). With the NPP_e value of each grid cell the percentages of change in NPP were derived by $100 * \text{tNPP} / \text{NPP}_e$, $100 * \text{cNPP} / \text{NPP}_e$ and $100 * \text{nNPP} / \text{NPP}_e$ and illustrated in Figures 5–7.

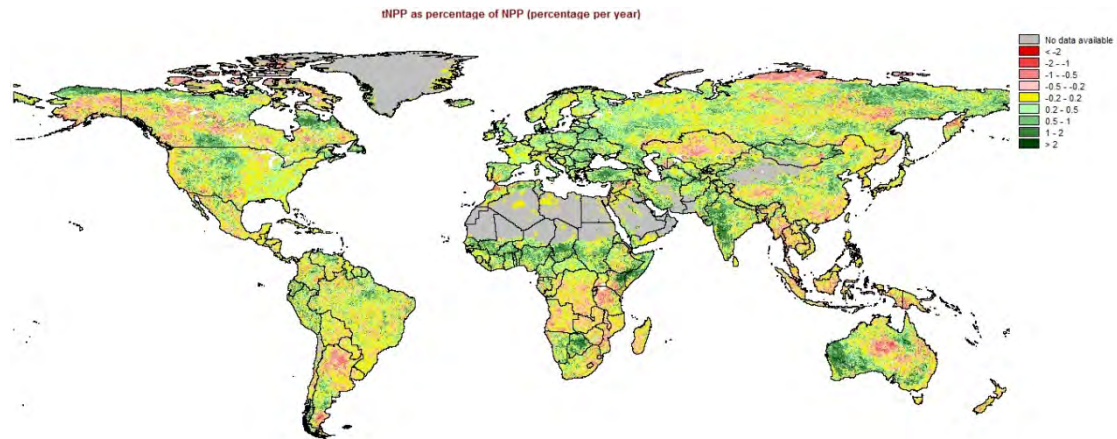


Figure 5

Actual change of estimated mean NPP (expressed as percentage per year) for the period 1981–2006.

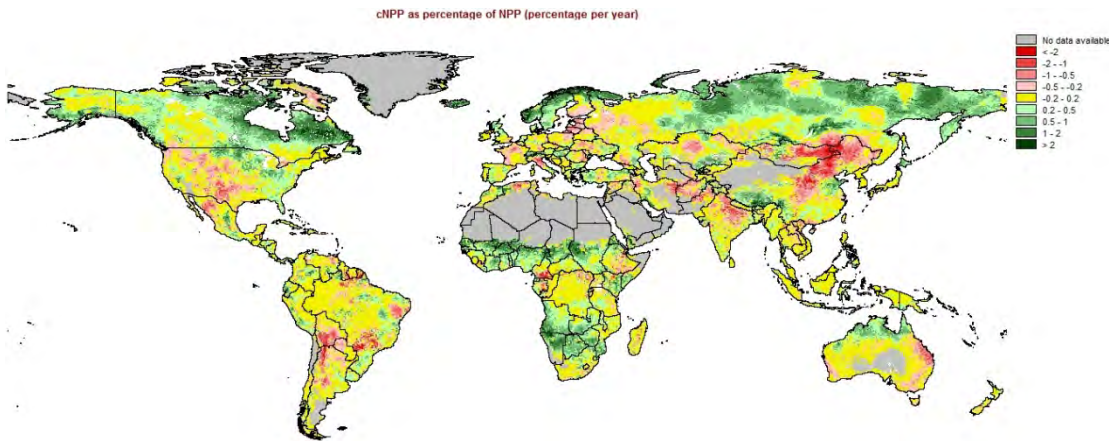


Figure 6
Climate-induced change of estimated mean NPP (expressed as percentage per year) for the period 1981–2006.

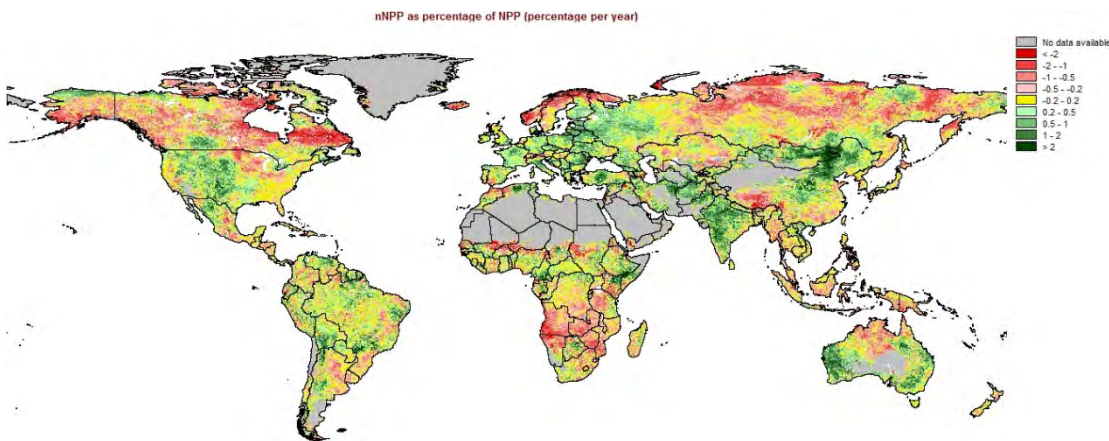


Figure 7
Non-climate related part of actual change of estimated mean NPP (expressed as percentage per year) for the period 1981–2006.

Comparing Figure 5 from this report with Figure 3 from Bai and colleagues (2012), depicting the relative changes in Σ NDVI, shows that both maps are similar in magnitude and sign of the illustrated variables which is caused by relation 3 linking the actual change in NPP to the change in Σ NDVI. Likewise, Figure 6 (this report) resembles Figure 6 of Bai *et al.* (2012) due to relation 4 where the change in NPP expected from changes in climate is estimated as function of the calculated change in TBW. The difference between actual and climate-induced change of NPP (Figure 7) is used to estimate the NPP change which cannot be attributed to changes in climate and is thus strongly affected by the difference in (relative) changes of Σ NDVI and TBW. *E.g.* in the Sahel zone (notably Mali, Burkina Faso and Niger) the Σ NDVI results indicate a '(re)greening' during 1981–2006 while TBW is also increasing due to improved weather conditions. Combining both data results in a negative change (declining trend) of the non-climate related NPP change, which could indicate that soil degradation may occur in this region, contrary to the first impression from the trend in Σ NDVI. In general there is a high correlation between positive values of the climate-induced NPP change (Figure 6) and negative values for the non-climate related NPP change (Figure 7) and vice versa with Figures 6 and 7 being 'mirror images' as a result (to a large extent). This is caused by the relative TBW change exceeding the relative Σ NDVI change in many grid cells, if expressed in absolute units (with positive values: relative TBW change > relative Σ NDVI change and with negative values: relative TBW change < relative Σ NDVI change).

5 Model sensitivity analysis

An analysis has been performed to investigate the sensitivity of the model output as function of model input. The aim of this sensitivity analysis is to determine for a limited number of model inputs, related to crop characteristics/management, whether the estimation of the climate-induced NPP change in section 4 is biased due to the model input used in calculating TBW (Bai *et al.*, 2012). Two model outputs have been selected for this analysis: average TBW (t DM ha⁻¹ y⁻¹) of the period 1981–2006 and 100*TBW_{slope} / TBW (= c%TBW in % y⁻¹) where TBW_{slope} is found by linear regression of annual TBW values on time (n=26 from 1981–2006). The quotient TBW_{slope} / TBW represents the relative change per year in TBW caused by climatic differences during 1981–2006. This output is considered in this sensitivity analysis because it affects the overall analysis and outcome of the NPP change maps (Figures 6 & 7) in this study.

The sensitivity analysis in this study is limited to *Miscanthus* and consequently covers most vegetated land (section 3.1). The simulation model is run for ca. 500,000 unique combinations of climate and soil characteristics (derived from the global gridded datasets) and these results were used in the sensitivity analysis. Due to the quotient TBW_{slope} / TBW, model results with a value of zero for the average TBW could not be used in the sensitivity analysis. Obviously, these zero values have been taken into account when processing the model results into the global gridded maps of TBW.

5.1 Standard run of *Miscanthus*

For the standard run of *Miscanthus* that has been used in Bai *et al.* (2012), the cumulative frequency distributions of both TBW and c%TBW are illustrated in Figure 8. Mean value for TBW is 26.5 t DM ha⁻¹ y⁻¹ and 90% of all values is below 66.2 t DM ha⁻¹ y⁻¹. Mean value for c%TBW is 0.191% y⁻¹ and 90% of all values lies between -2.92% y⁻¹ and +2.96% y⁻¹. For the positive values of c%TBW, the mean amounts 1.15% y⁻¹ and 90% is below 2.49% y⁻¹ and for the negative values the mean equals -1.55% y⁻¹ and 90% is above -4.13% y⁻¹ (see also Table 2). Next to the slope also the standard deviation of the slope has been computed; the quotient of slope and standard deviation of the slope gives the t-value and values below -2.06 and above 2.06 indicate statistically significant slopes (n = 26; p < 0.05). It can be concluded that ca. 85.5% of all results have a t-value between -2.06 and +2.06 and that these slopes are not significantly different from zero if an uncertainty of 5% is adopted. With a higher level of uncertainty (p < 0.10), 22.5% of all data is significantly different from zero and the remaining 77.5% is not (Figure 9).

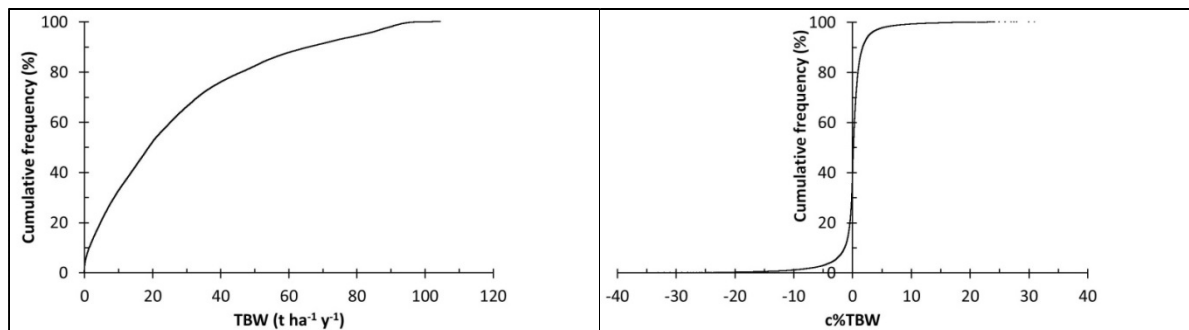


Figure 8

Cumulative frequency distribution of (a) TBW and (b) c%TBW of the standard run of *Miscanthus* for all unique climate-soil combinations with average TBW > 0 (n = 404,085).

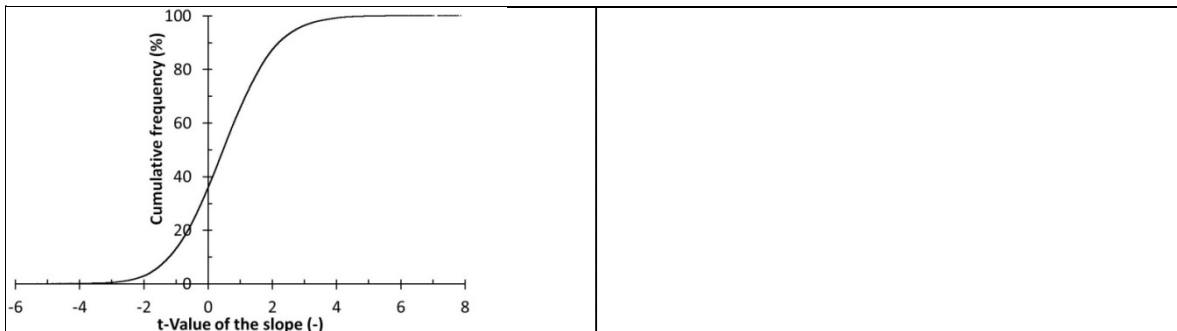


Figure 9

Cumulative frequency distribution of the *t*-value of the slope of the standard run of *Miscanthus* for all unique climate-soil combinations with average TBW > 0 and standard deviation of slope > 0 (*n* = 404,067).

In Figure 10a, c%TBW is plotted against TBW and shows that the higher values of c%TBW (either positive or negative) are found at lower values of TBW. Climate and soil conditions that ‘produce’ high average TBW values tend to have lower relative change rates which could indicate a higher stability in productivity (for a complete analysis of this stability also other variables should be examined, such as the standard deviation of the mean).

In the model growth conditions are evaluated for each year (1981–2006) to determine whether a crop can grow or not. A crop cannot grow when it is too cold or too dry during most of the year. The model results for a specific soil-climate combination can thus consist of 26 times of ‘zero-growth’ (*e.g.* in a desert) up to 26 times of ‘growth’ (*e.g.* in a tropical rainforest). In our analysis the average TBW of 1981–2006 is based on all 26 values, including the years with ‘zero-growth’ and due the limitation that average TBW > 0, at least one year in the sensitivity analysis was suitable for crop growth according to the model. Table 1 contains some data of the occurrence of ‘growth’ years: for 72% of the results all years were suitable for growth, for 86% the number of suitable years was at least 20 and situations with only 1 or 2 suitable years occurred in 2.5% of the results. It was expected that the absolute value of c%TBW is negatively correlated to the number of suitable years (see Figure 10). This can be explained by the generally lower average TBW and higher variability of annual TBW values when more years have a zero growth. Figure 10b shows that 19 or more suitable growth years (*ca.* 87% of the data) have values for c%TBW between –10% and +10% per year which implies that higher (more positive or negative) values of c%TBW only occur when 8 or more years were not suitable for growth.

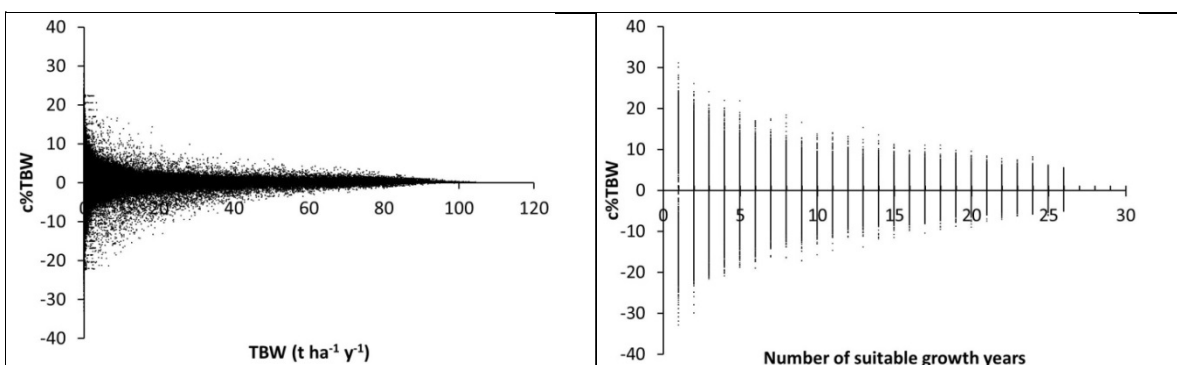


Figure 10

Relation between (a - left) c%TBW and TBW and (b - right) c%TBW and number of suitable years within the period 1981–2006 for the standard run of *Miscanthus* (average TBW > 0; *n* = 404,085).

Table 1

Cumulative percentage of the number of years with/without growth within 1981–2006 for the standard run of *Miscanthus* and average TBW > 0 (maximum number = 26).

No. of years with growth	No. of years without growth	Percentage (n = 404,085)
1 or 2	25 or 24	2.5
1 – 13	More than 12	10
1 – 19	More than 6	14
1 – 25	More than 0	28
26	0	72

In the model precipitation affects the results in two ways. First, precipitation determines with other factors the length of the growth period, which may be zero if conditions are too dry. Second, in the growth period precipitation affects crop transpiration and thereby possible water stress on growth resulting in lower production rates relative to the situation with irrigation in the growth period. To investigate the effects of precipitation, average TBW has been plotted against average cumulative precipitation during the growth period (PreGP, mm) and c%TBW has been plotted against the relative change in cumulative precipitation during the growth period (c%PreGP = $100 * \text{PreGP}_{\text{slope}} / \text{PreGP}$; compare c%TBW) for each run (see Figure 11).

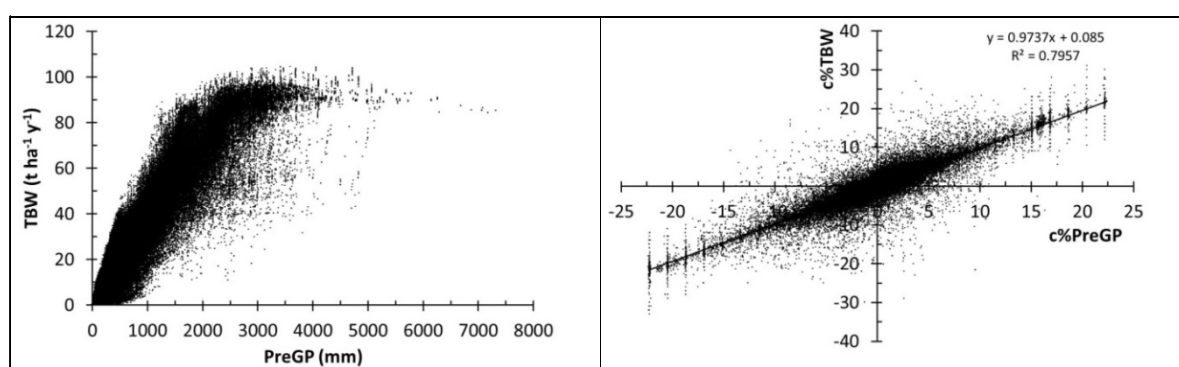


Figure 11

Relation between (a) average TBW and cumulative precipitation in the growth period (PreGP) and between (b) c%TBW and c%PreGP during 1981–2006 of the standard run of *Miscanthus* (average TBW > 0; n = 404,085).

Average cumulative precipitation during the growth period appears to be a good predictor of average TBW (90% of the variance can be explained by an exponential curve; F pr. < 0.001) and the relative change in PreGP is closely correlated to the relative change in TBW (Figure 11b; in a linear regression 80% of the variance is explained). On average a change in c%PreGP correlates with an almost equal change in c%TBW and in most situations, i.e. 81.1% of all data, an increasing cumulative precipitation in the growth period during 1981–2006 is related to an increase in TBW and vice versa. This indicates that c%TBW is closely related to the length of the growth period in days and its average daily precipitation (product of both equals PreGP) for the period 1981–2006.

5.2 Irrigated run of Miscanthus

The first example of alternative input refers to the situation with irrigation during the growth period to reduce the water stress during this period to zero. It was hypothesized that irrigation would decrease the relative changes in TBW because weather variability would be reduced by adding extra water. In the model this option does not affect the length of the growth period, which depends on precipitation before and near the end of the growth period, next to other factors, such as temperature. Figure 12 illustrates the effects on average TBW and c%TBW and shows that the average TBW is increased (all values are equal or larger than those from the standard run) where the absolute value of c%TBW is on average lower than in the standard run. However, there still remains a large amount of variation in c%TBW of the irrigated run which means that irrigation in the growth period only has a limited effect on the values of c%TBW as calculated in the standard run.

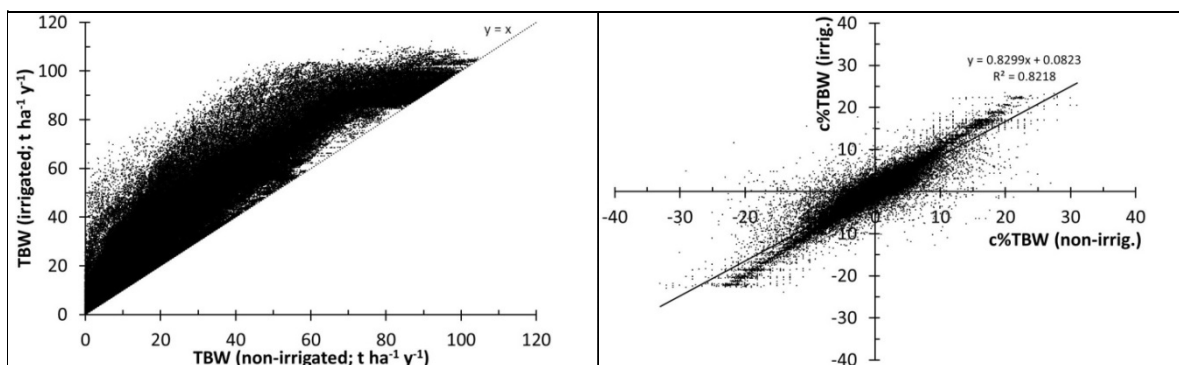


Figure 12

Relation between (a – left) TBW and (b – right) c%TBW of the irrigated run and the standard (= non-irrigated) run of Miscanthus (average TBW > 0; $n = 404,085$).

5.3 Run with red=0.5 for Miscanthus

Two input parameters have been adjusted simultaneously: a reduction factor of 0.5 is introduced that is multiplied in the model with both the biomass production as well as the leaf area growth on a daily basis (in the standard run this factor equals 1.0, *i.e.* no reduction) and the maximum leaf area index (LAI) is reduced with 50% relative to its original value of the standard run. This option was selected because it was hypothesized that in the simulated rain-fed growing conditions assuming *e.g.* ample nutrient supply and consequently higher production levels than can be expected in reality under nutrient limited conditions, the effect of weather variability on TBW would be amplified. Using the reduction factor as explained above introduces an extra limiting factor causing lower biomass production in the model and expected lower sensitivity to weather variability. Figure 13 illustrates the effects on average TBW and c%TBW and shows that the average TBW is reduced with ca. 53% (slightly higher than the reduction factor) and that on average c%TBW is equal to the standard run, indicating that the slope of TBW of this new run is also reduced with ca. 53%. When both the average and the slope are reduced with the same magnitude the c%TBW will not be different as is the case in this run compared to the standard run. The introduction of the reduction factor, as described above, to calculate lower (more realistic) TBW values did not affect the relative changes in TBW compared to the standard run and the hypothesis of the effects of weather variability 'being amplified' in the standard run has not been confirmed.

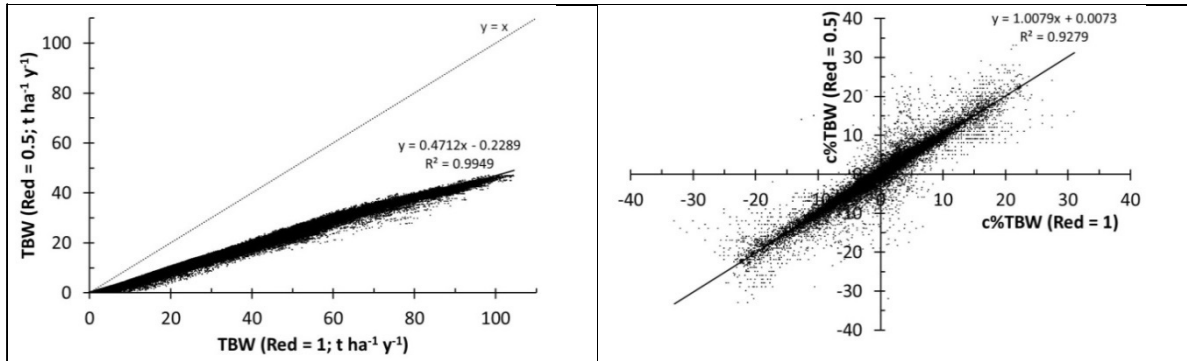


Figure 13

Relation between (a – left) TBW and (b – right) c%TBW of the run with red=0.5 and the standard run of Miscanthus (average TBW > 0; n = 404,085).

5.4 Reed canary grass

Reed canary grass has been used in the sensitivity analysis as an alternative perennial species and being a C3 species many crop characteristics differ from Miscanthus (C4 species). In general it will better adapted to colder environments and has a lower production in warmer/drier climates. The effects on average TBW and c%TBW are illustrated in Figure 14.

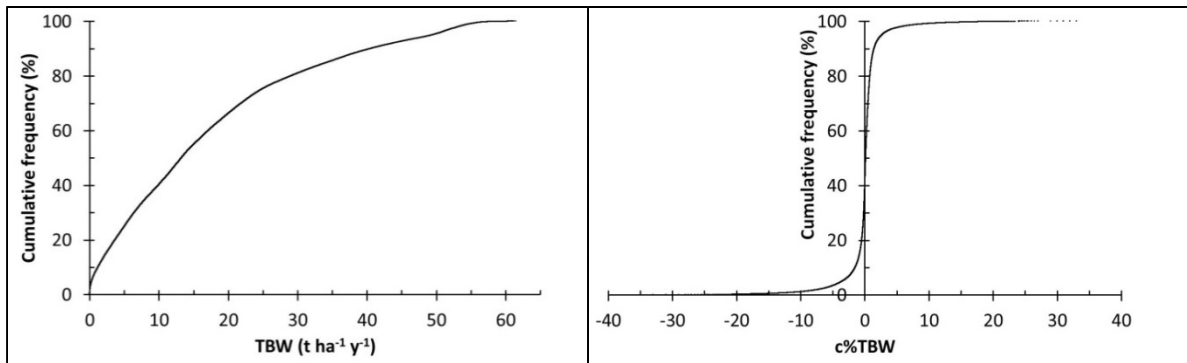


Figure 14

Cumulative frequency distribution of (a – left) TBW and (b) c%TBW (b – right) of the run of Reed Canary grass for all unique climate-soil combinations with average TBW > 0 (n = 396,393).

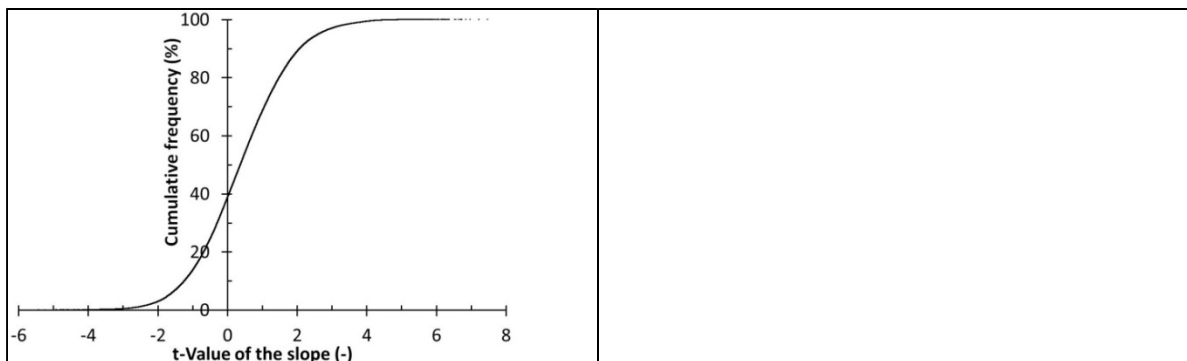


Figure 15

Cumulative frequency distribution of the t-value of the slope of the run of Reed Canary grass for all unique climate-soil combinations with average TBW > 0 (n = 396,393).

Mean value for TBW is 17.0 t DM ha⁻¹ y⁻¹ and 90% of all values is below 40.5 t DM ha⁻¹ y⁻¹. Mean value for c%TBW is 0.04% y⁻¹ and 90% of all values lies between -3.50% y⁻¹ and +2.68% y⁻¹. For the positive values of c%TBW, the mean amounts 1.08% y⁻¹ and 90% is below 2.22% y⁻¹ and for the negative values the mean equals -1.63% y⁻¹ and 90% is above -4.46% y⁻¹. Table 2 contains the data next to the run with Miscanthus. Based on the t-values of Reed canary grass (Figure 15) it can be concluded that ca. 87.1% of all results have a t-value between -2.06 and +2.06 and that these slopes are not significantly different from zero if an uncertainty of 5% is adopted. With a higher level of uncertainty (p < 0.10), 20.6% of all data is significantly different from zero and the remaining 79.4% is not (Figure 15).

Table 2

Some data on mean TBW and mean c%TBW.

Run	mean TBW	90%_TBW	mean c%TBW	90%_limits	positive mean c%TBW	90%_pos. c%TBW	negative mean c%TBW	90%_neg. c%TBW
Miscanthus n=404,085	26.5	66.2	0.191	-2.92<>+2.96	1.15	2.49	-1.55	-4.13
Reed C.grass n=396,393	17.0	40.5	0.04	-3.50<>+2,68	1.08	2.22	-1.63	-4.46

90%_TBW = TBW value below which 90% of the data occurs

90%_limits = negative and positive c%TBW values between which 90% of the data occurs

90%_pos. c%TBW = for positive c%TBW values, the c%TBW value below which 90% of the data occurs

90%_neg. c%TBW = for negative c%TBW values, the c%TBW value above which 90% of the data occurs

These results show that the average TBW values of Reed Canary grass are significantly lower than those of Miscanthus (Table 2) and that the %cTBW values are comparable to those from Miscanthus. The large difference in TBW is accompanied by a relatively equal difference in the slope values, i.e. sensitivity to weather variability, which results in similar %cTBW values.

Table 3

Cumulative percentage of the number of years with growth within 1981–2006 for the run with Reed canary grass and average TBW > 0 (maximum number = 26).

No of years with growth	No of years without growth	Percentage (n = 396,393)
1 or 2	25 or 24	2.4
1 – 13	More than 12	10
1 – 19	More than 6	14
1 – 25	More than 0	29
26	0	71

Summarizing, the calculated mean TBW is strongly affected by the changes in model input. Using Reed canary grass instead of Miscanthus or introducing a growth reduction factor both decreased the mean TBW considerably while on the other hand applying irrigation in the growing season increased the mean TBW. However, using another (C3) perennial grass species or altering the production level by introducing the reduction factor had practically no effect and irrigation had only a very modest effect on the relative change in

TBW which was calculated from the annual weather data during 1981–2006. Referring to the aim of this sensitivity analysis, alternative crop model input that would significantly affect the outcome of the climate-related NPP change maps (Figures 6 and 7) was not found in this study. With respect to the investigated model input, the calculations of the relative change in TBW from Bai and colleagues (2012) are rather robust.

6 Detecting abrupt changes in NDVI

Land degradation is driving long-term losses of ecosystem functioning. Global changes of satellite measurements of vegetation greenness (NDVI) since 1981 have been determined in the previous study (Bai *et al.*, 2012). However, these changes in greenness, based on time series of NDVI, leave abrupt changes undetected. These abrupt changes might have occurred *e.g.* because of changes in land use and directly affecting the NDVI values but they are not necessarily related to soil degradation such as forest fires. Degradation is expected to result in more gradual changes.

Global time series are not available for changes in land use. This hampers direct analyses of abrupt changes in land use at the global scale. We therefore selected twenty locations in four regions around the world with known changes in land use for instance from forest to agriculture, re- and deforested areas, wildfire and without land use change in the same area in order to

- 1) illustrate variations in Σ NDVI of these locations for 1981–2006;
- 2) analyze whether it would be possible to identify a threshold to trace the disturbances compared to the locations without disturbances;
- 3) explore whether or not abrupt NDVI change can be detected through the threshold method;
- 4) test whether the thresholds can be verified in other sites and applied globally.

In addition, data of global abrupt NDVI trend changes during 1982–2008 by de Jong *et al.* (2012) were referenced as supplementary information for these case by case analyses.

6.1 NDVI variations in areas with/without LUC in the Argentinean Chaco region

Land use change in the Chaco region of Argentina since 1977 has been detected by mapping parcels where the original vegetation has been substituted by crops in four temporal series 1977, 1992, 2002, 2008 (Bai *et al.*, 2013, Figure 16, left) and five sites in the polygon maps with known land use change and without land use change are selected for analysis of NDVI variations. Additionally global abrupt trend change of NDVI detected by de Jong *et al.* (2012) for the Chaco region are shown in Figure 16, right; Σ NDVI variations for the selected sites with/without land use changes are presented in Figure 17 and summarized in Table 4.

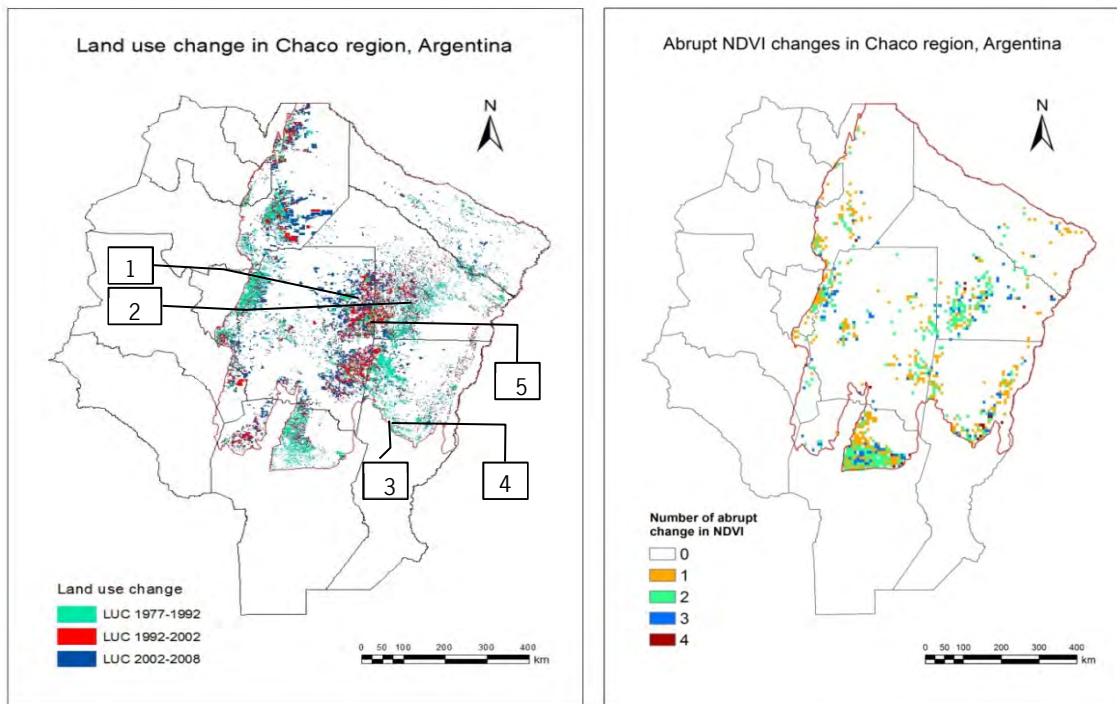


Figure 16
 Land use change (left, data from Adámoli et al., 2011, 1-5 are the selected sites) and abrupt trend change in NDVI (right, data from de Jong et al., 2012) in the Chaco region.

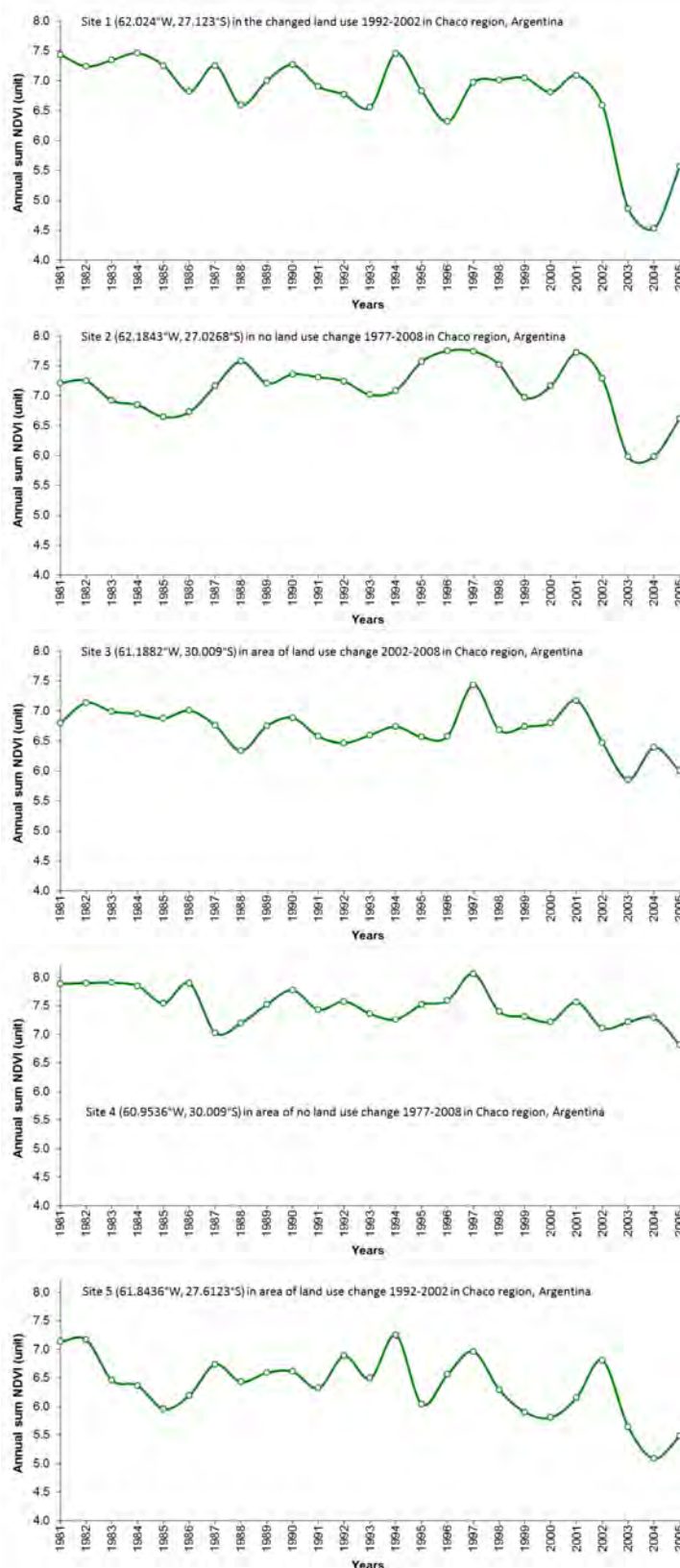


Figure 17

ΣNDVI variations 1981–2006 with/without LUC in the Chaco region, Argentina (five sites, based on the LUC map made by Adámoli et al., 2011).

At site 1, land cover is a mosaic vegetation comprising 50–70% of mixed grassland, shrub land and forest and 20–50% cropland. Land use changed from forest to cropland during 1992–2002. Multi-year mean Σ NDVI is 6.76, standard deviation is 0.75. The difference between multi-year mean Σ NDVI and the lowest value of Σ NDVI (in the year 2004) is 2.23. There is no abrupt NDVI trend change detected according to the data analysed by de Jong *et al.* (2012).

Site 2 is adjacent to site 1: land cover is closed (>40%) broadleaved deciduous forest (>5m); no land use change occurred during 1977–2008. Multi-year mean Σ NDVI is 7.11, standard deviation is 0.47. The difference between multi-year mean Σ NDVI and the lowest value of Σ NDVI (in the year 2003) is 1.14. There is no abrupt NDVI trend change detected by de Jong *et al.* (2012).

At site 3, land cover is comparable to site 1. Land use changed during 2002–2008. Multi-year mean Σ NDVI is 6.70, standard deviation is 0.35. The difference between multi-year mean Σ NDVI and the lowest value of Σ NDVI (in the year 2003) is 0.85. One abrupt NDVI trend change was detected according to de Jong *et al.* (2012).

Site 4 is adjacent to site 3. Land cover is closed to open with >15% (broadleaved or needle-leaved, evergreen or deciduous) shrub land (<5m). No land use change occurred during 1977–2008. Multi-year mean Σ NDVI is 7.49, standard deviation is 0.32. The difference between multi-year mean Σ NDVI and the lowest value of Σ NDVI is 0.68. There is no abrupt NDVI trend change detected by de Jong *et al.* (2012).

At site 5, land cover comprises rain-fed croplands, whereas land use changed during 1992–2002. Multi-year mean Σ NDVI is 6.37, standard deviation for the changes in land use is 0.55. The difference between multi-year mean Σ NDVI and the lowest value of Σ NDVI (in the year 2004) is 1.29. Two abrupt NDVI trend changes were detected by de Jong *et al.* (2012).

The results for the above-mentioned sites are summarized in Table 4.

Table 4
Statistics of NDVI, land cover and LUC at five sites in the Chaco region, Argentina.

Sites	Lon/Lat (degree)	Land cover (ESA, 2008)	LUC ¹	Σ NDVI _{avg} ²	Σ NDVI _{stdev} ³	Σ NDVI _{avg} - Σ NDVI _{min} ⁴	$\frac{100(\Sigma\text{NDVI}_{\text{avg}} - \Sigma\text{NDVI}_{\text{min}})}{\Sigma\text{NDVI}_{\text{avg}}}$	Abrupt NDVI change ⁵
1	62.024W/27.123S	Mosaic vegetation (grassland shrubland forest) (50-70%) cropland (20-50%)	yes	6.7594	0.7489	2.2307	33.0	0
2	62.1843W/27.0268S	Closed (> 40%) broadleaved deciduous forest (>5m)	no	7.1147	0.4682	1.1362	16.0	1
3	61.1882W/30.009S	Mosaic vegetation (grassland shrubland forest) (50-70%) cropland (20-50%)	yes	6.7021	0.3467	0.8451	12.6	1
4	60.9536W/30.009S	Closed to open (>15%) (broadleaved or needle-leaved, evergreen or deciduous) shrubland (<5m)	no	7.4909	0.3183	0.6784	9.1	0
5	61.8436W/27.6123S	Rain-fed croplands	yes	6.3733	0.5396	1.2866	20.2	2

¹ LUC = land use change

² NDVI_{avg} = Multi-year mean Σ NDVI (1981-2006)

³ NDVI_{stdev} = Multi-year Σ NDVI standard deviation (1981-2006)

⁴ NDVI_{min} = Multi-year minimum Σ NDVI (1981-2006)

⁵ Number of abrupt trend change in NDVI (1981-2006) (according to de Jong *et al.* 2012)

In the Chaco region, 95% of the changes in land use refer to changes of forest or grassland into cropland (Bai *et al.*, 2013). Figure 17 and Table 4 indicate that i) the changes in land use from forest or grassland to cropland result in the reduction in greenness, *i.e.*, average Σ NDVI; ii) the largest drops of the Σ NDVI did not occur in the known periods of land use changes (site 1 and 5); iii) there are differences in the standard deviation of the average Σ NDVI for sites with land use change (sites 1 and 5) and without land use change (sites 2 and 4) but there are also no obvious differences between the site with LUC (site 3) and the sites without LUC (sites 2 and 4); iv) the average of the differences between multi-year average Σ NDVI and minimum Σ NDVI for the three sites with land use changes is 1.454.

The difference between multi-year average Σ NDVI and minimum Σ NDVI might be an indicator for any changes in land use but the value for this threshold remains to be tested. A tentative threshold value of 1.454 (see above) is applied both to the global scale (a draft map is appended in Appendix I; Figure A1) and to the Chaco region (Figure 18, left). Comparison of Figure 18 (left) to Figure 16 (left) indicated that some 26.3% of the cells with a value larger than this threshold show changes in land use coincidentally; the remaining cells (73.7%) with a value larger than 1.454 show no changes in land use. In contrast, 24.5% of the areas with changes in land use (Figure 16 (left)) are detected by the indicator (*i.e.* difference between multi-year average and minimum Σ NDVI) if the value of 1.454 is used as threshold. The average value of the indicator for all the areas (pixels) with known land use changes in the Chaco region is 1.185. If this lower threshold value is used, some 23.8% of all pixels with a value larger than 1.185 in the Chaco region also show land use change and 46.1% of all cells with land use change have a value larger than 1.185.

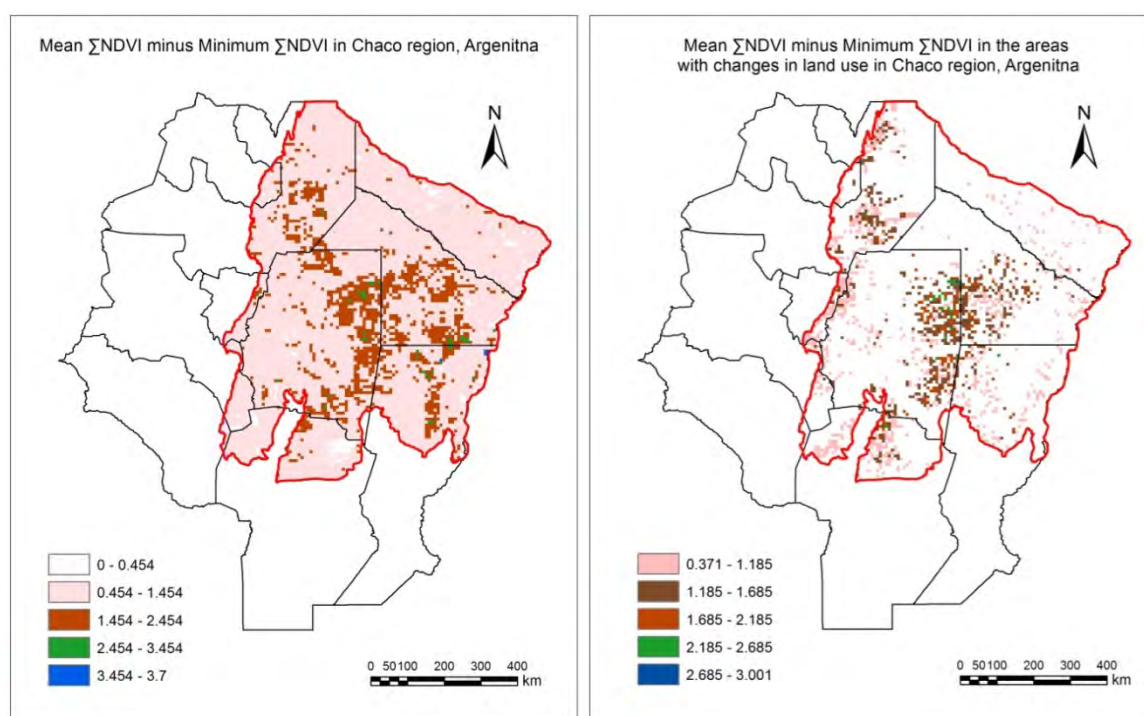


Figure 18

Difference between multi-year mean Σ NDVI and minimum Σ NDVI for the Chaco region (left, ≥ 1.454) and for the areas with changes in land use (right, average value ≥ 1.185).

A relative deviation, *i.e.*, the ratio between the difference of the multi-year mean annual Σ NDVI and minimum Σ NDVI and the multi-year mean annual Σ NDVI, or $100(\Sigma\text{NDVI}_{\text{avg}} - \Sigma\text{NDVI}_{\text{min}})/\Sigma\text{NDVI}_{\text{avg}}$ was calculated for all cells. A value of 20% is used as a threshold based on the ratios at the selected sites where the land use changes

were known. Figure 19 (left) shows the areas where the relative deviation is larger than this threshold. Statistics show that 24% of the grid cells with the relative deviation larger than the threshold (20%) experienced land use change. The global values for this relative deviation during 1981–2006 are illustrated in Figure A2 in the Appendix I.

Standard deviation of annual Σ NDVI over 1981–2006 was calculated for the selected sites (Table 4), the average of annual Σ NDVI standard deviation for the sites with land use change is 0.55. Statistics indicates that 26.3% of the grid cells in the Chaco region with the standard deviation larger than 0.55 experienced land use change (Figure 19, right). The global values for the Σ NDVI standard deviation during 1981–2006 are illustrated in Figure A3 in the Appendix I.

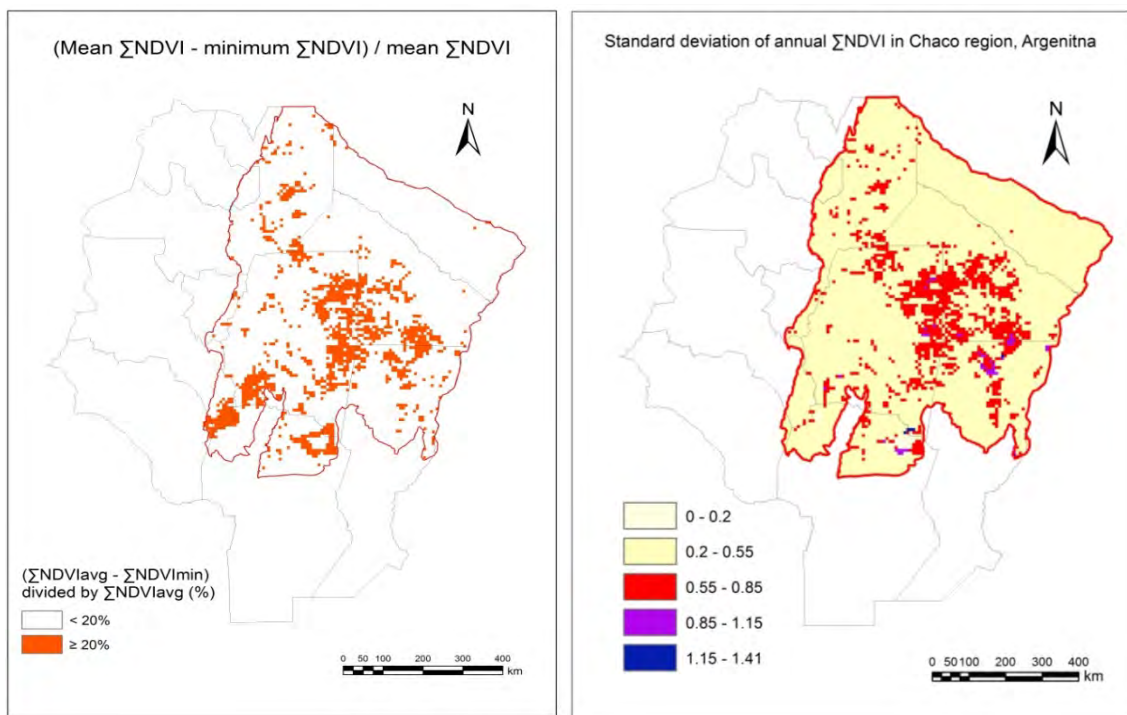


Figure 19
 Percentage of Σ NDVI_{avg} - Σ NDVI_{min} / Σ NDVI_{avg} larger than 20% (left), standard deviation of annual Σ NDVI (right) in the Chaco region, Argentina.

6.2 NDVI variations in the areas with/without LUC in the Argentinean Salta province

To match the period of NDVI time series 1981–2006, land use change for the same period for Salta province of Argentina are determined (Figure 20 (left, data from Adámoli *et al.*, 2011)). This period also fits well with the abrupt NDVI trend change detected by de Jong *et al.* (2012; Figure 20, right). Land use change in this case consists of a change from forest to crop land. NDVI variations at the four sites (two sites with LUC; and two without LUC) are illustrated in Figure 21, statistics are summarized in Table 5.

At site 1: land use changed during 1981–2006 and current land is covered by rain-fed crops; multi-year mean annual sum NDVI (Σ NDVI) is 6.04, standard deviation is 0.44. The difference between multi-year mean Σ NDVI and the lowest value of Σ NDVI (in the year 2001) is 1.09; One abrupt NDVI change was detected according to de Jong *et al.* (2012).

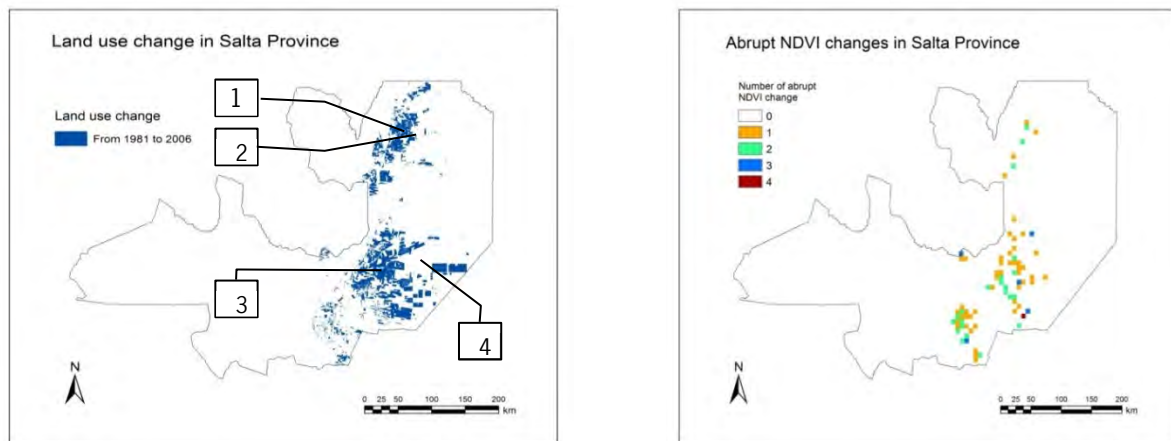


Figure 20

Land use change during 1981–2006 (left, 1–5 are the selected sites) and abrupt trend in NDVI (right) in Salta province, Argentina.

Site 2 is adjacent to site 1 without land use change, land cover is closed (>40%) broadleaved deciduous forest (>5m) (ESA, 2008). Multi-year mean annual sum NDVI is 6.81, standard deviation is 0.41. The difference between multi-year mean Σ NDVI and the lowest value of Σ NDVI (in the year 1982) is 0.81; no abrupt NDVI change was detected according to de Jong *et al.* (2012).

At site 3: land use changed during 1981–2006, current cover consists of rain-fed crops; multi-year mean Σ NDVI is 5.60, standard deviation is 0.38. The difference between multi-year mean Σ NDVI and the lowest value of Σ NDVI (in the year 2004) is 0.87; One abrupt NDVI change was detected according to Rogier *et al.* (2012).

At site 4: there was no land use change, land is covered by a closed (>40%) broadleaved deciduous forest (>5m) (ESA, 2008). Multi-year mean annual sum NDVI is 6.77, standard deviation is 0.54. The difference between multi-year mean Σ NDVI and the lowest value of Σ NDVI (in the year 2004) is 1.29; no abrupt NDVI change was detected according to Rogier *et al.* (2012).

Table 5

Statistics of NDVI, land cover and LUC of four sites in the Salta province, Argentina.

Sites	Lon/Lat (degree)	Land cover (ESA, 2008)	LUC ¹	Σ NDVI _{avg} ²	Σ NDVI _{stdev} ³	$\frac{\Sigma$ NDVI _{avg} - \SigmaNDVI_{min}⁴}	$100(\frac{\Sigma$ NDVI _{avg} - \SigmaNDVI_{min}) / \SigmaNDVI_{avg} change⁵}}	Abrupt NDVI
1	63.647W/22.764S	Rain-fed cropland	yes	6.0363	0.4391	1.094	18.12	1
2	63.4349W/22.7953S	Closed (>40%) broadleaved deciduous forest (>5m)	no	6.8131	0.4098	0.8071	11.85	0
3	63.9511W/24.8486S	Rain-fed cropland	yes	5.8977	0.379	0.8738	14.82	1
4	63.3613W/24.6695S	Closed (>40%) broadleaved deciduous (>5m)	no	6.7743	0.5354	1.2943	19.11	0

¹ LUC = land use change

² NDVI_{avg} = Multi-year mean Σ NDVI (1981-2006)

³ NDVI_{stdev} = Multi-year Σ NDVI standard deviation (1981-2006)

⁴ NDVI_{min} = Multi-year minimum Σ NDVI (1981-2006)

⁵ Number of abrupt trend change in NDVI (1981-2006) (according to de Jong *et al.* 2012)

In the Salta province, multi-year average Σ NDVI for the cropland sites (1 and 3) is close to 6 which is about 0.8 lower than that for the broadleaved deciduous forest sites (2 and 4; Table 5); the differences of the multi-year average Σ NDVI for the sites with/without LUC are hardly distinguished; this is also true for the standard deviation of the annual Σ NDVI and for the difference between multi-year mean Σ NDVI and lowest Σ NDVI values. A threshold cannot be identified from this case analysis.

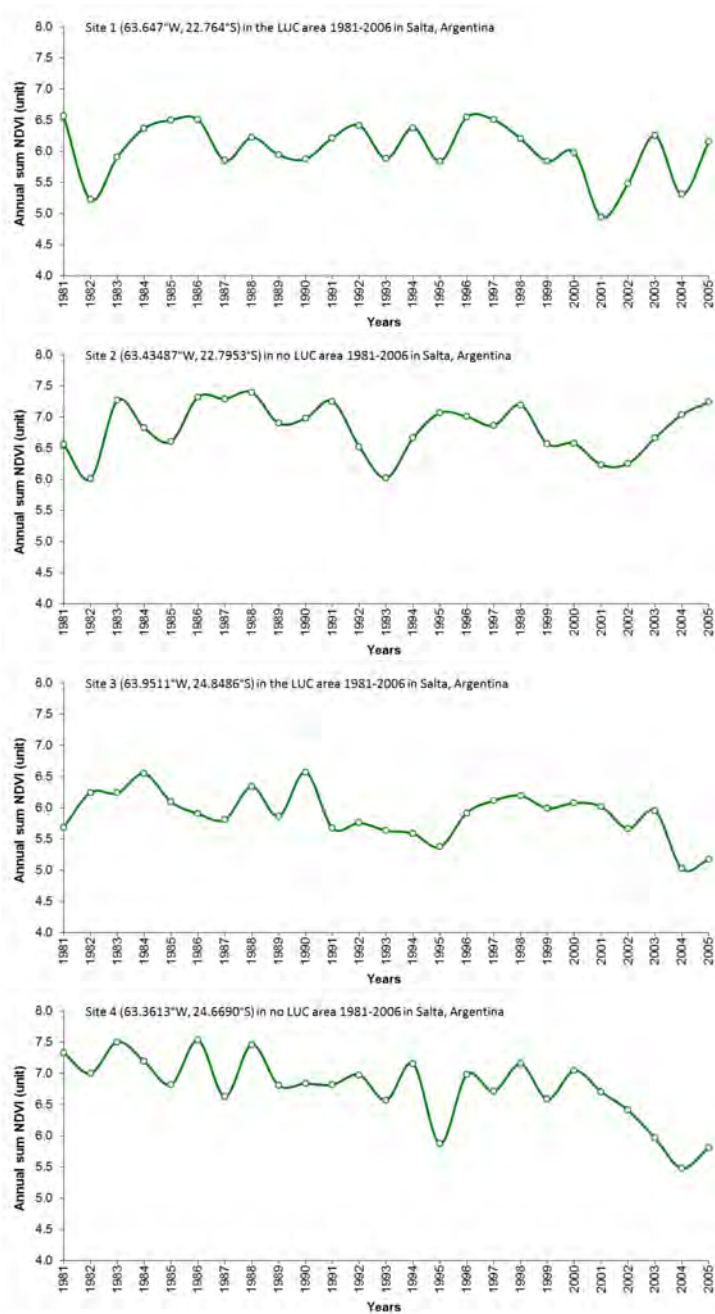


Figure 21
 NDVI variations 1981–2006 at sites with/without LUC indicated in the headings of each graphs in the Salta province, Argentina.

6.3 NDVI variations in burnt and non-burnt areas in the Southeastern Russia

Wild fire in south-east (SE) Russia for the period of 1996–2002 has been determined by the Satellite image analysis (Sukhinin *et al.*, 2004). The burnt areas were double checked with *GLC2000* Global Land Cover data (JRC, 2006). Figure 22 shows the time series areas burnt per year and Figure 23 illustrates the inventory of the burning (top) and abrupt NDVI trend change according to de Jong *et al.* (2012).

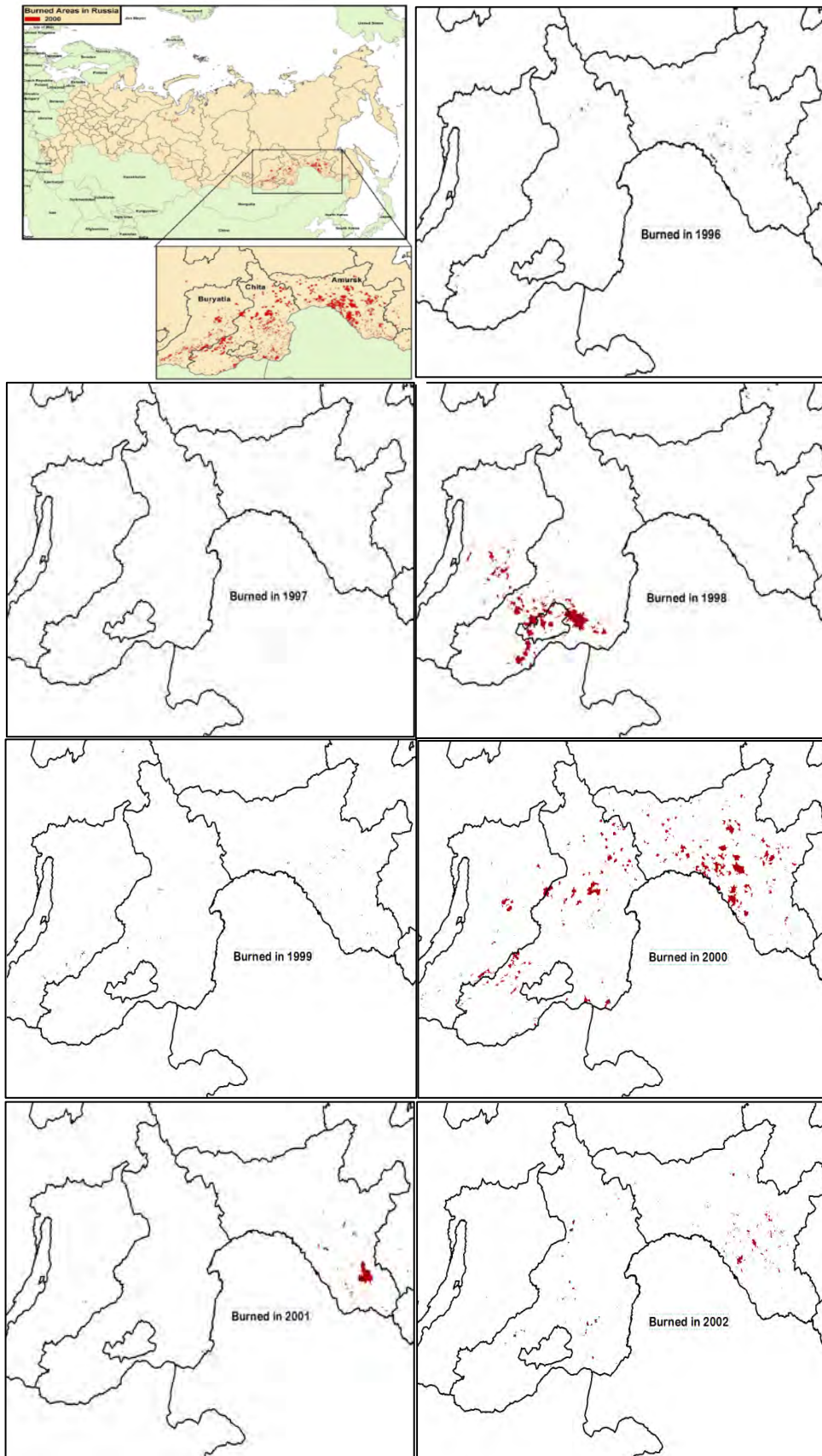


Figure 22
 Wildfire in SE Russia from 1996 to 2002.

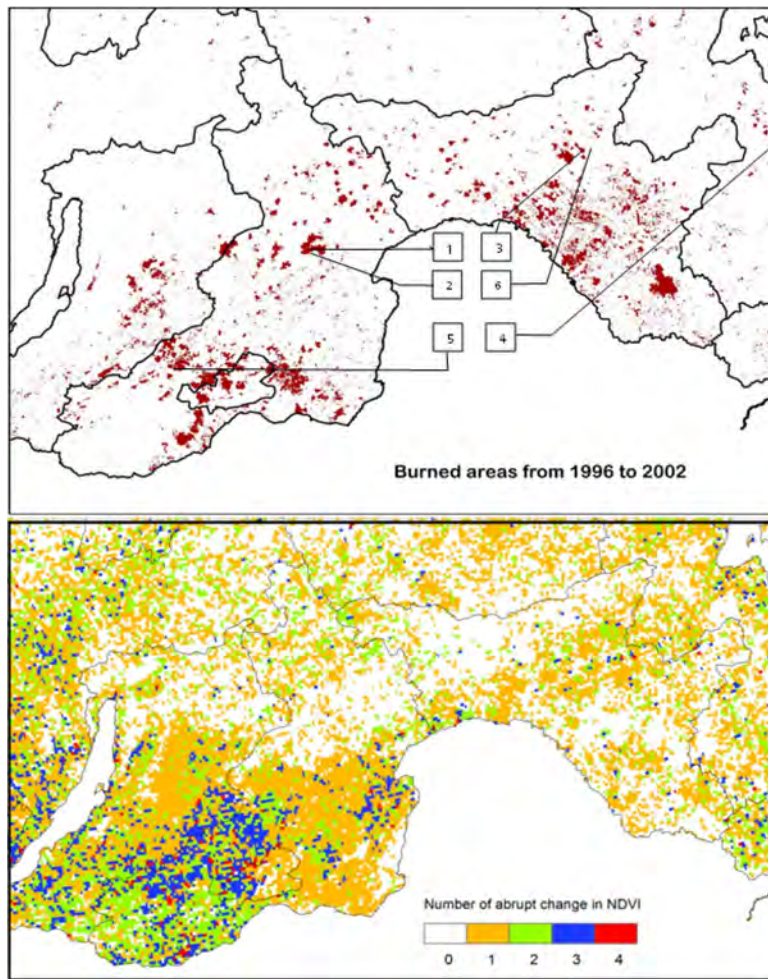
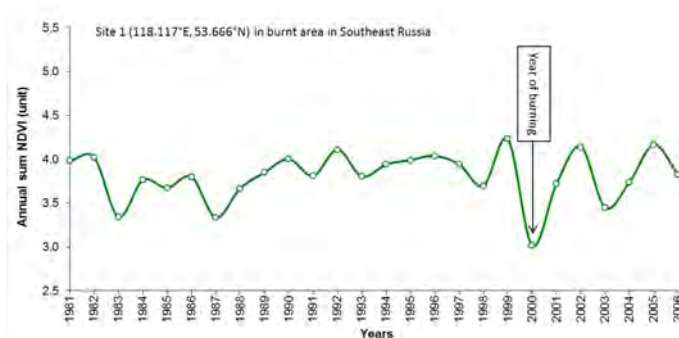


Figure 23

Top: aggregation of areas affected by wildfire events for the period of 1996–2002; sites 1–6 are the selected sites; bottom: abrupt trend change in NDVI over 1982–2008 (de Jong et al., 2012).

Figure 24 shows variations of annual Σ NDVI over 1981–2006 at sites in the burnt and no burnt areas in SE Russia; their statistics are summarized in Table 6.



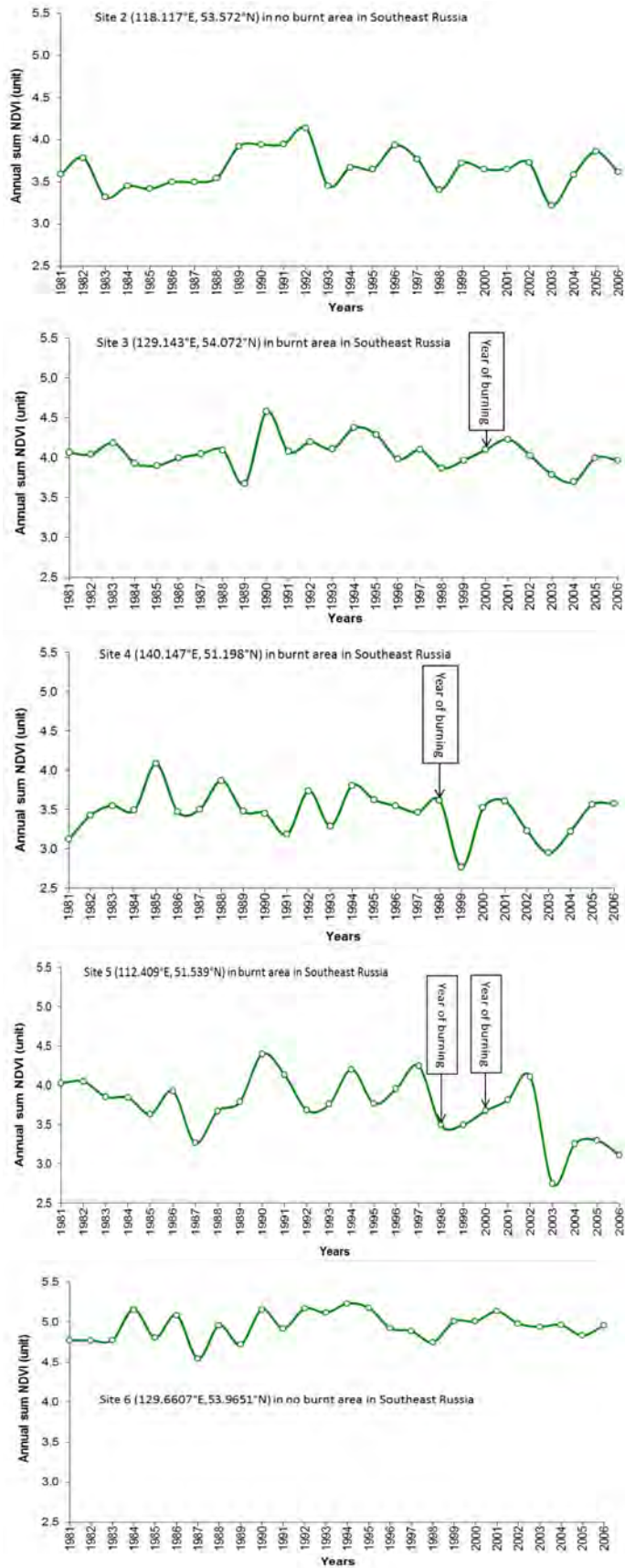


Figure 24
ΣNDVI variations in the burnt and no burnt areas in SE Russia.

Site 1 was initially covered by needle-leaved, deciduous forest (JRC, 2000) and wildfire occurred in the year 2000 (Sukhinin *et al.*, 2004). The multi-year mean Σ NDVI is 3.81; the Σ NDVI value after burning is 0.79 lower than the multi-year mean; the standard deviation of annual Σ NDVI values for the entire period 1981–2006 is about 0.28. One abrupt NDVI trend change was detected by de Jong *et al.* (2012) for the site. After two years the vegetation seems to have recovered in terms of Σ NDVI values.

Site 2 shows NDVI variation in a non-burnt area in SE Russia, adjacent to site 1; land is covered by a needle-leaved, deciduous forest (JRC, 2000). The standard deviation of the annual Σ NDVI values over 1981–2006 is 0.22 and multi-year mean of Σ NDVI is 3.65; the difference between multiyear mean Σ NDVI and minimum Σ NDVI is 0.43. There is one abrupt trend change detected according to de Jong *et al.* (2012).

At site 3 initial cover consisted of a needle-leaved, deciduous forest (JRC, 2000) and wildfire occurred in the year 2000. Multi-year mean Σ NDVI is 4.05; standard deviation of annual Σ NDVI values is 0.19; the difference between multi-year mean Σ NDVI and minimum Σ NDVI is 0.38. No abrupt NDVI trend change was detected by de Jong *et al.* (2012).

Site 4 was covered by trees and burnt in 1998. Multi-year mean Σ NDVI is 3.47; standard deviation of annual Σ NDVI values is 0.28. The difference between multi-year mean Σ NDVI and minimum Σ NDVI is 0.70. One abrupt NDVI trend change was detected by de Jong *et al.* (2012).

Site 5 was covered by trees and burnt in 1998 and 2000. Multi-year mean Σ NDVI is 3.74; standard deviation is 0.38; the difference between multi-year mean Σ NDVI and minimum Σ NDVI is 0.99. Three abrupt NDVI trend changes were detected by de Jong *et al.* (2012).

Site 6 refers to non-burnt area and is covered by needle-leaved evergreen forest; multi-year mean Σ NDVI is 4.95 with a standard deviation of 0.173; the difference between multi-year mean Σ NDVI and minimum Σ NDVI is 0.41. One abrupt NDVI trend change was detected by de Jong *et al.* (2012).

Table 6
Statistics of NDVI in the burnt and non-burnt areas in Southeast Russia.

Sites	Lon/Lat (degree)	Land cover (JRC, 2000)	Burnt ¹	Σ NDVI _{avg} ²	Σ NDVI _{stdev} ³	Σ NDVI _{avg} - Σ NDVI _{min} ⁴	$\frac{100(\Sigma$ NDVI _{avg} - Σ NDVI _{min})}{\SigmaNDVI_{avg}}}}	Abrupt NDVI change ⁵
1	118.117E/53.666N	Burnt area (Code=10)	yes	3.8104	0.2833	0.7934	20.82	1
2	118.117E/53.572N	Needleleaved, deciduous forest	no	4.0475	0.1946	0.375	9.26	1
3	129.143E/54.072N	Burnt area (Code=10)	yes	3.6543	0.2191	0.4287	11.73	0
4	140.147E/51.198N	Burnt area (Code=10)	yes	3.4669	0.2789	0.7034	20.29	1
5	112.409E/51.539N	Burnt area (Code=10)	yes	3.7371	0.3826	0.9911	26.52	3
6	129.661°E/53.965°N	Needleleaved evergreen forest	no	4.9544	0.1728	0.4084	8.24	1

¹ According to Sukhinin *et al.*, 2004

² NDVI_{avg} = Multi-year mean Σ NDVI (1981-2006)

³ NDVI_{stdev} = Multi-year Σ NDVI standard deviation (1981-2006)

⁴ NDVI_{min} = Multi-year minimum Σ NDVI (1981-2006)

⁵ Number of abrupt trend change in NDVI (1981-2006) (according to de Jong *et al.* 2012)

Table 6 and Figure 24 indicate that i) multi-year mean Σ NDVI for the burnt areas is lower than that for the non-burnt areas (comparing site 1 to site 2 which had similar land cover before the burning, or site 3 to site 6 which had similar land cover before the burning), the difference is approximately 0.83; ii) the Σ NDVI at the burnt sites either recovered within 2–3 years after burning (sites 1 and 4), or showed no obvious change before and after burning (site 3 and 2nd burning at site 5); iii) the Σ NDVI standard deviation for the burnt areas is higher than those for the non-burnt areas, the difference is about 0.11; iv) the difference between multi-year mean Σ NDVI and minimum Σ NDVI is higher for the burnt areas than for the non-burnt areas, the difference is about 0.34.

6.4 NDVI variations in areas with/without deforestation in the DR of the Congo

Satellite images on forest cover and change for the periods of 2000–2005 and 2005–2010 in the Democratic Republic of the Congo (OSFAC, 2010) was downloaded and displayed in Figure 25. The Landsat Enhanced Thematic Mapper Plus (ETM+) images with less than 50% cloud cover were processed to generate the forest cover extent and loss analysis for 2000 to 2005 and 2005 to 2010. The ETM+ data are resampled to a 60 m spatial resolution. Forest was defined as 30% or greater canopy cover for trees of 5 meters or more in height. All such assemblages that were converted to non-forest are quantified and labelled as forest cover loss. Forest cover and loss were divided into three categories: primary forest, secondary forest and woodlands. Primary forest cover is defined as mature forest with greater than 60% canopy cover. Secondary forest is defined as re-growing immature forest with greater than 60% canopy cover. Woodland is defined as forest cover with greater than 30% and less or equal to 60% canopy cover. Permanent water bodies were mapped separately (OSFAC, 2010).

The forest cover and loss for the period of 2000–2005 is used for this case analysis. Figure 26 shows the details through zooming in and is used to extract time series NDVI for the selected sites (Figure 27); the results are summarized in Table 7.

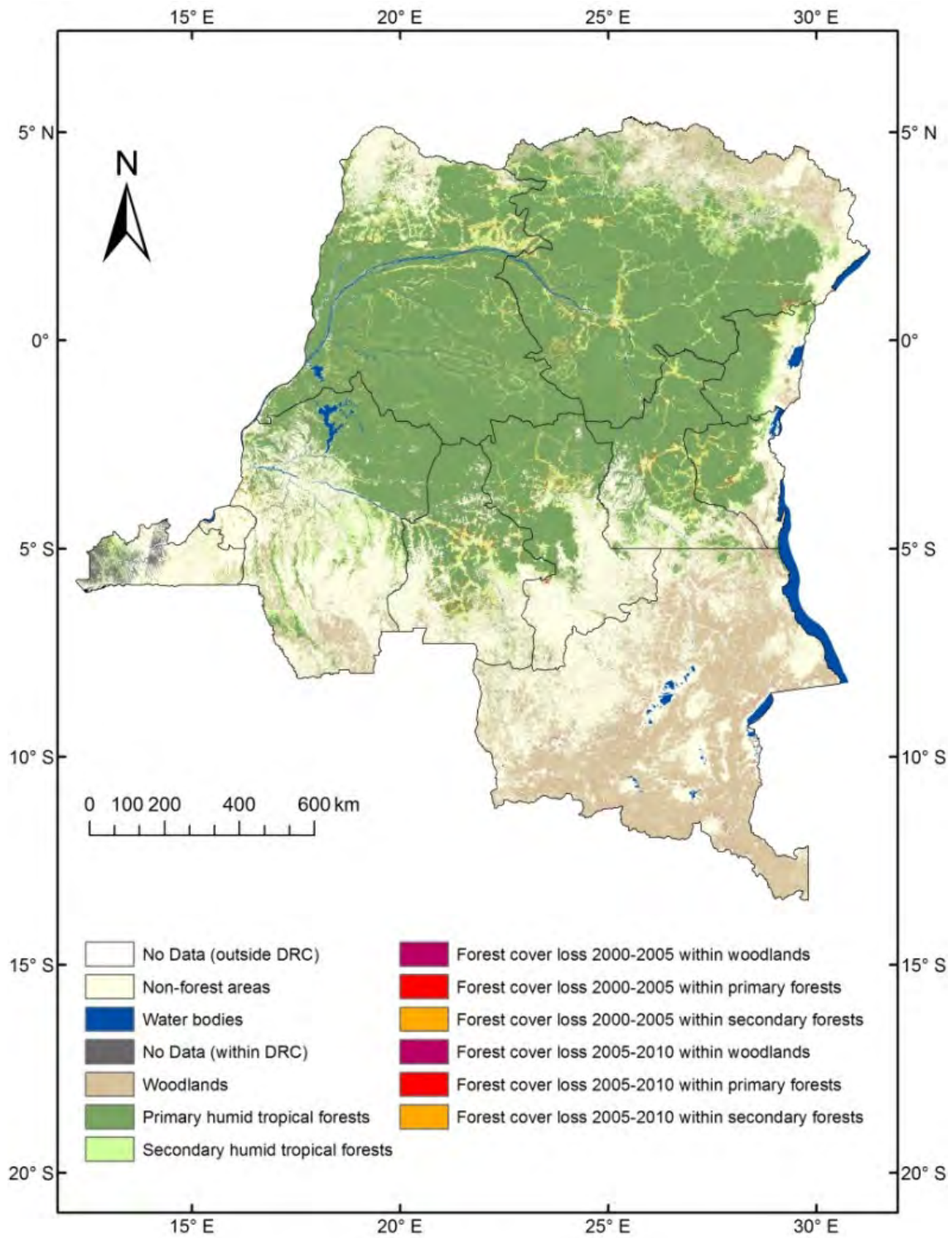


Figure 25
Forest cover and loss within 2000–2005 and 2005–2010 in the DR of the Congo.

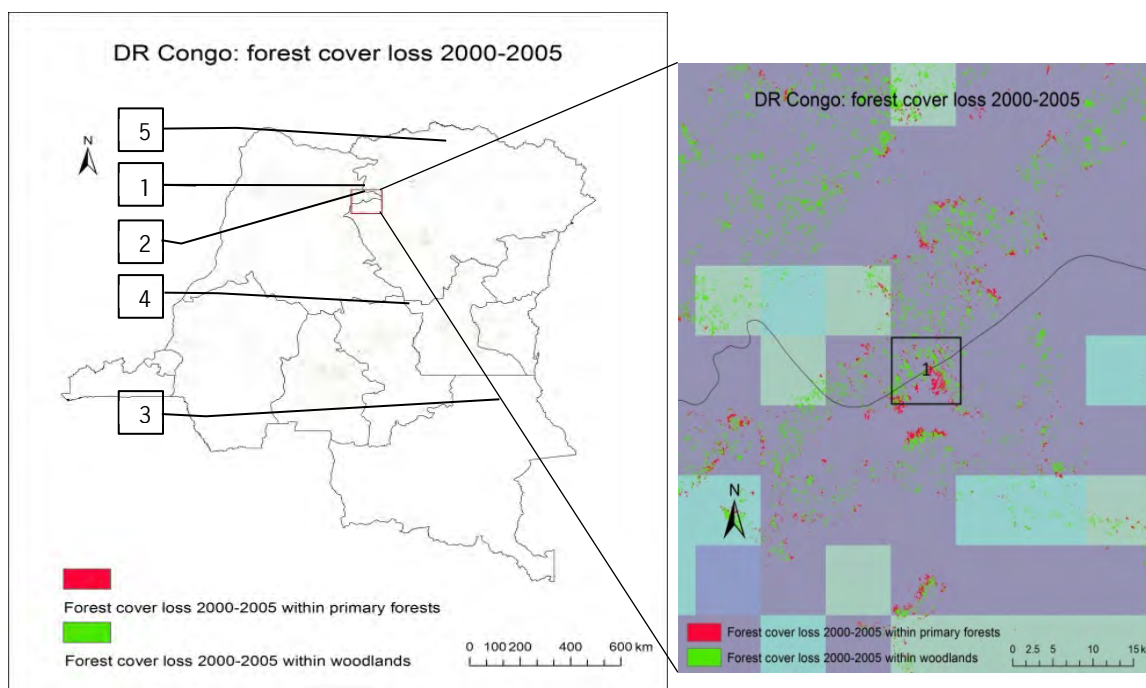


Figure 26

Forest cover loss within 2000–2005 in a part of the DR of the Congo, 1–5 are the selected sites.

At site 1, land cover is primary humid tropical forest with about 30% deforestation by area during 2000–2005; multi-year mean Σ NDVI is 8.52; standard deviation is 0.34; the difference between multi-year mean Σ NDVI and minimum Σ NDVI is 0.58. No abrupt NDVI trend changes were detected by de Jong *et al.* (2012) for this site.

Site 2 is close to site 1 but land cover is 100% primary humid tropical forest; there is no deforestation; multi-year mean of Σ NDVI is 8.63; standard deviation is 0.31; the difference between multi-year mean Σ NDVI and minimum Σ NDVI is 0.53. no abrupt NDVI trend changes were detected by de Jong *et al.* (2012).

Site 3: land cover is woodlands without deforestation. Multi-year mean of Σ NDVI is 7.46; standard deviation is 0.25; the difference between multi-year mean Σ NDVI and minimum Σ NDVI is 0.64. No abrupt NDVI trend changes were detected by de Jong *et al.* (2012).

It is hard to find forest cover loss in the woodlands dominated area during 2000–2005.

Site 4: land cover is secondary humid tropical forests with about 20% deforestation by area during 2000–2005. Multi-year mean of Σ NDVI is 8.74; standard deviation is 0.54; the difference between multi-year mean Σ NDVI and minimum Σ NDVI is 0.85. Two abrupt NDVI trend changes were detected by de Jong *et al.* (2012).

Site 5: land cover is secondary humid tropical forests without deforestation. Multi-year mean of Σ NDVI is 9.11; standard deviation is 0.27; the difference between multi-year mean Σ NDVI and minimum Σ NDVI is 0.67. One abrupt NDVI trend change was detected by de Jong *et al.* (2012).

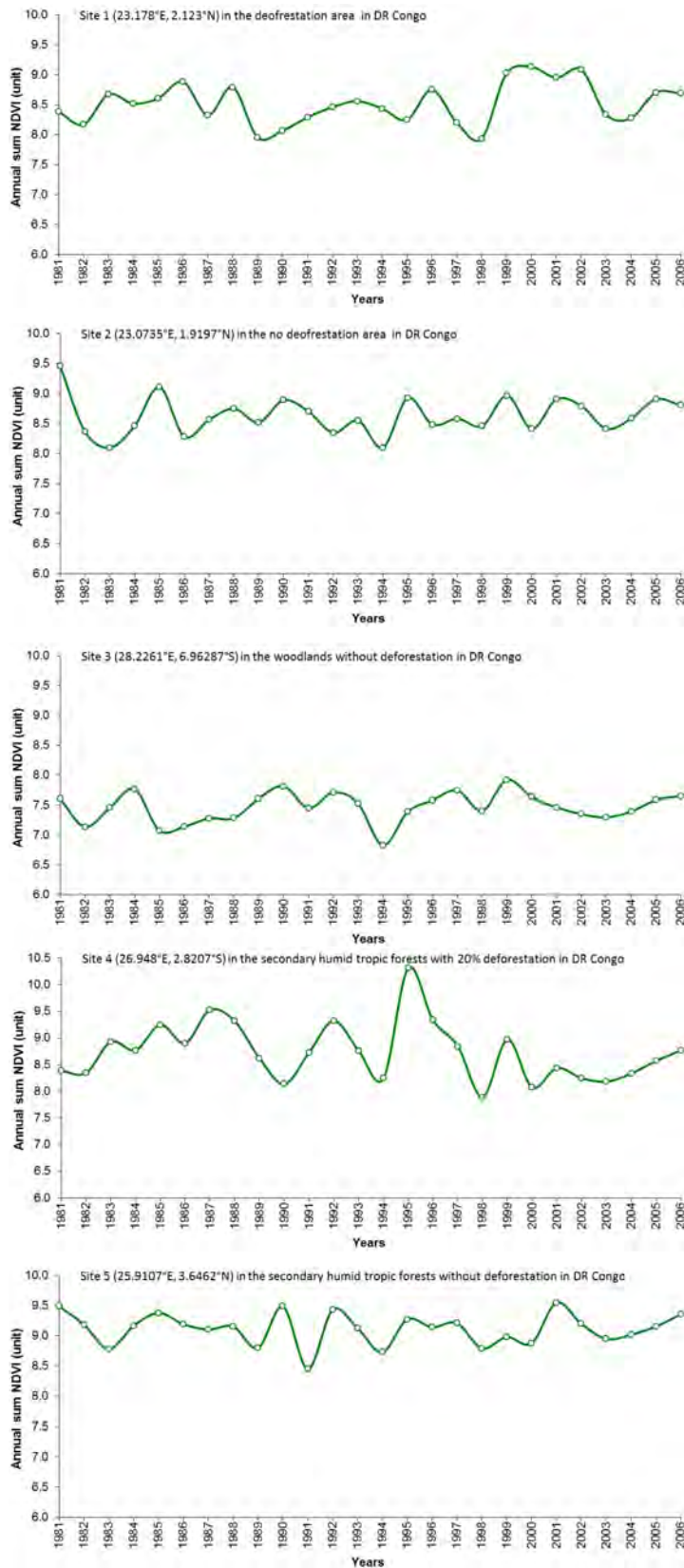


Figure 27
NDVI variations in the areas with/without forest loss in the DR of the Congo.

Table 7*Statistics of NDVI in the areas with/without forest loss in the DR of the Congo.*

Sites	Lon/Lat (degree)	Land cover (OSFAC, 2010)	Deforestation ¹	$\Sigma\text{NDVI}_{\text{avg}}$ ²	$\Sigma\text{NDVI}_{\text{stdev}}$ ³	$\Sigma\text{NDVI}_{\text{avg}} - \Sigma\text{NDVI}_{\text{min}}$ ⁴	$\frac{100(\Sigma\text{NDVI}_{\text{avg}} - \Sigma\text{NDVI}_{\text{min}})}{\Sigma\text{NDVI}_{\text{avg}}}$	Abrupt NDVI change ⁵
1	23.178E/2.123N	Primary humid tropic forests	30%	8.5179	0.3385	0.5824	6.84	0
2	23.0735E/1.9197N	Primary humid tropic forests	no	8.6319	0.3131	0.5341	6.19	0
3	28.2261E/6.9629S	Woodlands	no	7.4641	0.2501	0.6357	8.52	0
4	24.948E/2.8207S	Secondary humid tropic forests	20%	8.7399	0.5445	0.8472	9.69	2
5	25.9107E/3.6462N	Secondary humid tropic forests	no	9.1137	0.2664	0.6657	7.30	1

¹ According to OSFAC, 2010² NDVI_{avg} = Multi-year mean ΣNDVI (1981-2006)³ $\text{NDVI}_{\text{stdev}}$ = Multi-year ΣNDVI standard deviation (1981-2006)⁴ NDVI_{min} = Multi-year minimum ΣNDVI (1981-2006)⁵ Number of abrupt trend change in NDVI (1981-2006) (according to de Jong *et al.* 2012)

Comparison of the multi-year mean ΣNDVI for the period of 1981–2006 at site 1 (deforestation) with that at site 2 (no deforestation) indicates that they are not significantly different; this is also true for the mean ΣNDVI during 2000–2005 in which deforestation occurred (mean ΣNDVI 8.75 for site 1 and 8.67 for site 2). Non-significant differences also occur between the (non-)deforested sites with respect to the difference between multi-year average ΣNDVI and minimum ΣNDVI (sites 1 and 2). The average difference in standard deviation of the annual ΣNDVI values between the sites with/without forest loss is 0.165.

7 Discussion and conclusions

In the previous study of Bai *et al.* (2012) and in this study, global changes of remotely sensed greenness (NDVI) and simulated biomass production (TBW) since 1981 have been analysed for the purpose of mapping global soil degradation. The overall objective of the research is to identify areas (grid cells) affected by soil degradation which can be used as input for the PBL project 'Biodiversity, Ecosystem services and Development' to assess the effects of land degradation on future economic development and biodiversity around the world (using the global model IMAGE). The impact of climate and human interventions causing abrupt changes like de- or reforestation has been examined/quantified in a global context. Ultimately, by combining Figure 7, illustrating the non-climate related part of actual changes of estimated mean NPP, with Figure A2 (Appendix I), illustrating areas with abrupt NDVI changes as indicator for abrupt land use changes, and by taking statistically significant changes of both NDVI and TBW into account (Figures 1 & 2) areas can be identified that were exposed to land degradation/improvement. Other factors that cause land degradation/improvement fell outside the scope of the two studies and the results are therefore only the first steps in mapping land degradation. Results will be verified in a related project by comparing changes in NDVI and TBW with local expert judgment from selected countries/areas. In this section the methodology to assess the loss of productivity by soil degradation, as developed in this study, is discussed and options for additional analyses and possible improvements are identified.

In the preparation of the final maps of NDVI, TBW and NPP, the grid cells which were assumed non-vegetated according to MODIS during 2000–2006, have been excluded, making these cells 'invisible' for the current analysis. We do suggest however to perform an additional study to analyze the temporal NDVI dynamics of these grid cells, because a negative change would indicate that these areas may have been vegetated at the earlier stage of the period 1981–2006 but lost their vegetation towards the end. Vice versa, a positive change may point at a re-greening area which may become more vegetated in the future if the positive trend continues. Such an exploration could reveal vulnerable areas.

Calculated annual TBW values vary throughout the study period 1981–2006 as a result of varying weather conditions. For each grid cell the trend in TBW is estimated through linear regression of TBW on time and the *t*-values of the slopes were used to test the significance of the trends. Many slopes were not significantly different from zero (Figure 2), which is also supported by the results from the Miscanthus run in the sensitivity analysis (Figure 9). This outcome could result from the relatively short study period during which significant changes in weather may not have occurred or trends could not be detected due to the large inter-annual fluctuations. This can be investigated by performing linear regressions of a number of weather variables on time for each grid cell, comparable to the analysis with Σ NDVI and TBW in this study, and calculate the *t*-values of their slopes. If most trends in weather data that are used as input for the model are not significant, then this would explain that many calculated TBW changes during 1981–2006 are not significant.

The maps of the climate-induced and the non-climate related NPP change (Figures 6 & 7) being mirror images of each other for most grid cells raises questions about the estimations of the actual NPP change as function of Σ NDVI_{trend} and the climate-induced NPP change as function of TBW_{slope}. Both an underestimation of the actual NPP change by using too low values for the relative change in Σ NDVI and an overestimation of the climate-induced NPP change by using too high values for the relative change in TBW will cause this mirror effect. Although it cannot be concluded that the data of maps are wrongly estimated (for this they should be verified with independent data), possible causes of under- and overestimation will be discussed below. *Underestimation* of the actual NPP change may occur because Σ NDVI values as used in our study are based on the sum of a

more variable part related to greenness and a more constant part not related to greenness. The more constant part refers to NDVI from (bare) soils and not-producing biomass (e.g. yellow grasses during dry periods and trees without leaves during cold periods), whereas the more variable part relates to the green mass of a vegetation. NPP changes will be more related to changes in the variable part, i.e. the green mass, and less to the NDVI value from (bare) soils and non-producing biomass and therefore the correlation between NPP change and Σ NDVI change can be improved if only the NDVI values from the 'actual' greenness would be used. This will give higher values for the relative Σ NDVI changes but effects of this correction on the estimation of the actual and non-climate related NPP changes have not been explored in this study. We recommend to explore the possibilities of distinguishing between these two parts of the total observed NDVI value and recalculate the resulting NPP change maps.

The other cause of the mirror effect which relates to the *overestimation* of climate-induced NPP change, could be explained by the situation that the effects of weather on biomass production may be exaggerated because the model calculations refer to the rain-fed production level which is not limited by nutrient shortages, occurrence of weeds, pests and diseases, and suboptimal management. Such limitations may interact with the effects of weather on biomass production and may dampen changes in TBW related to changes in weather. Moreover, adaptation of a vegetation to changing weather conditions, e.g. other species, other characteristics, may also decrease the effect of a change in weather conditions compared to a non-adapted situation (which is used in the calculations where only the length of the growing season is adapted per year as function of the weather conditions). The sensitivity analysis in this study was aimed at searching for factors that influence the relative change in TBW (i.e. TBW_{slope}/TBW) to investigate options for improving the estimation of the climate-induced NPP change. Results of this analysis showed that using a C3 perennial species (Reed canary grass) instead of a C4 perennial (Miscanthus) did not significantly alter the relative change in TBW. This is also concluded for using a reduction factor in the model calculations to mimic nutrient limitations with consequently lower (more realistic) production levels. A correction of the current model calculations by including irrigated crop lands will also not lead to very different results in the relative TBW change (the effect of irrigation on relative TBW change of Miscanthus was small in the sensitivity analysis and the amount of irrigated crop land as percentage of total global land area is also small although it can be high in certain regions). Overall, we have not found indications that the current model calculations lead to an overestimation of climate-induced NPP changes. However, the explanation of the generally larger values of relative TBW change (compared to relative Σ NDVI change) needs further investigation to understand and check these values.

The model sensitivity analysis in chapter 5 shows that irrigation had only a modest effect on the relative change in TBW of Miscanthus (Figure 12b), while a strong correlation appeared between the relative change in TBW and the relative change in cumulative precipitation during the growing season (Figure 11b). These two results seem to contradict because irrigation decreases the variation in plant available water during the growing season and it was expected that this would also reduce the relative variability in TBW. However, besides a small decrease in relative TBW change, both TBW and the TBW_{slope} are affected relatively in a similar way, indicating that if the mean TBW increases with x % by irrigation, also the slope of the linear regression has increased with almost x %. This suggests that the strong correlation with cumulative precipitation mainly originates from a strong correlation with the length of the growing season which is defined by the start and the end. Besides suitable temperatures during the growing season (mainly being not too cold), the start of the growing season depends on sufficient soil moisture availability at the starting day and beyond which is strongly influenced by the (cumulative) precipitation prior to the starting day. On the other hand, the end day depends on soil moisture conditions becoming unfavourable for crop production and is therefore affected by (cumulative) precipitation towards the end of the growing season. The calculation of starts and ends and consequently the length of the growing season is performed without any contribution of (possible) irrigation to soil moisture and is therefore equal for rain-fed and irrigated situations in the model calculations. If variation in the length of the growing season is the main driver for variation in TBW, it would explain (a) the strong correlation of TBW with cumulative precipitation during the growing season because cumulative precipitation

will be positively affected by the length of the growing season and (b) also the modest effect of irrigation because irrigation does not affect the length of the growing season. This would suggest that the variation in TBW is significantly affected by weather conditions outside the growing season. To test this assumption on the cause of the variation in TBW some additional (statistical) analyses should be done.

Another option for investigating non-climate related changes in NPP can be studied by using all seven years of NPP data separately (2000–2006; in this report only the average values from this period have been used) and calculating the slope of NPP against time ($n = 7$) for each grid cell. These NPP slopes can be correlated to (a) $\Sigma\text{NDVI}_{\text{trend}}$ and (b) $\text{TBW}_{\text{slope}}$ (both then also calculated for 2000–2006) in two separate regressions linking the change in ΣNDVI and in TBW directly to the change in NPP (note: these slope calculations are now only based on 7 data points for each grid cell). It can be assumed (like in this study) that relations of 2000–2006 also apply to 1981–2006. Total change in NPP can be calculated as function of $\Sigma\text{NDVI}_{\text{trend}}$ of 1981–2006 and the relation between NPP slope and $\Sigma\text{NDVI}_{\text{trend}}$ from 2000–2006 and climate-induced part of the actual change in NPP can be found by $\text{TBW}_{\text{slope}}$ of 1981–2006 and the relation between NPP slope and $\text{TBW}_{\text{slope}}$ from 2000–2006. This procedure of direct correlation (NPP slope, $\Sigma\text{NDVI}_{\text{trend}}$ and $\text{TBW}_{\text{slope}}$) may avoid possible over- or underestimation of the non-climate related NPP changes, but the ‘disadvantage’ lies in the short period and consequently small amount of data points per grid cell that can be used for these correlations ($n = 7$), which makes it more difficult to produce significant changes due to changes in weather. This alternative analysis has not been done due to this disadvantage and the limited budget.

In this study a start has been made with developing a methodology towards mapping global soil degradation. It is assumed that soil degradation is a relatively slow process taking place during many years and that abrupt land use change occurs within a few years. Abrupt land use changes (such as caused by wildfire or deforestation) might be represented by negative values in Figure 7 (illustrating the non-climate related part of actual change of estimated mean NPP), but do not indicate soil degradation. It is assumed that abrupt land use changes correlate with abrupt changes in NDVI and therefore it is investigated in this study whether and how time series of annual ΣNDVI can be used to detect abrupt land use changes. For this purpose twenty locations around the world with known changes/no changes in land use were selected and corresponding time series of annual values of ΣNDVI from 1981 to 2006 were extracted from the global data set. These time series have been displayed for each location to illustrate any abrupt NDVI changes that can be linked to the known changes in land use, deforestation and wildfire.

Three variables based on annual ΣNDVI were calculated, *i.e.*, multi-year average annual ΣNDVI , minimum annual ΣNDVI and annual ΣNDVI standard deviation over the period of 1981–2006. The multi-year mean annual ΣNDVI values for the 20 selected sites are different: highest for the dense forest (average of 8.5 in the DRC case) and lowest for the needle-leaved forest and shrub (3.95 in the SE Russia case). The annual ΣNDVI values from 1981 to 2006 vary significantly with an average standard deviation of 0.371 ranging from 0.173 to 0.749; the differences between the multi-year mean annual ΣNDVI and minimum ΣNDVI vary for different land cover types from 0.375 to 2.231 with an average value of 0.861.

The difference between multi-year mean annual ΣNDVI and minimum annual ΣNDVI was initially calculated for the detection of abrupt NDVI changes. Results of a tentative threshold, *i.e.* ($\Sigma\text{NDVI}_{\text{avg}} - \Sigma\text{NDVI}_{\text{min}}$) ≥ 1.454 applied to the Chaco region, indicated that about one quarter of the grid cells with a difference larger than this threshold has the changes in land use. The multi-year mean annual ΣNDVI for the 20 selected sites vary with highest values for the dense forest and lowest values for needle-leaved forest and shrub and the differences between the multi-year mean annual ΣNDVI and minimum ΣNDVI also vary for different land cover types. Therefore, it is not recommended to obtain a threshold from these differences of the ‘absolute’ values and to apply this threshold to all land cover categories at the global scale, because the annual ΣNDVI of the different land cover types are different. It should only be applied to locations with homogeneous land cover and change, for example in the Chaco region of Argentina where 95% of the land use change are from forest to crop. As an

alternative option the ratio between the difference of the multi-year mean annual Σ NDVI and minimum Σ NDVI and the multi-year mean annual Σ NDVI, *i.e.*, $100(\Sigma\text{NDVI}_{\text{avg}} - \Sigma\text{NDVI}_{\text{min}})/\Sigma\text{NDVI}_{\text{avg}}$ was calculated for each location, and a ratio of 20% is tentatively set as threshold. Results from this threshold of $100(\Sigma\text{NDVI}_{\text{avg}} - \Sigma\text{NDVI}_{\text{min}})/\Sigma\text{NDVI}_{\text{avg}}$ applied to the Chaco region indicated that about 24% of the grid cells with a ratio larger than this threshold have the changes in land use.

The global abrupt NDVI trend change by de Jong *et al.* (2012) was detected using fortnightly time series from 1982 to 2008 and many abrupt changes were found around large-scale natural influences like the Mt Pinatubo eruption in 1991 and the strong 1997/98 El Niño event. Yet, it is difficult to compare this abrupt NDVI change with global consistent time series data on land use changes for the period of 1981–2006 which are not available or not compatible with the GIMMS data period. Comparison of the known changes in land use at the selected sites (20) with the abrupt NDVI trend change by de Jong *et al.* (2012) indicates that 8 out of 11 sites with known land use change show the abrupt NDVI trend change and 5 of the 9 sites without land use change show no abrupt NDVI trend change. For the annual NDVI data from this study and using the ratio as indicator with 20% as threshold, the results of detection are: 5 out of 11 sites and 9 out of 9 sites.

However there are some inherent limitations using GIMMS NDVI dataset to detect changes in land use at either fortnightly or annual footprint: (1) the coarse spatial resolution of the NDVI dataset: an $8 \times 8 \text{ km}^2$ pixel integrates the signal from a wider surrounding area, while changes in land use or deforestation rarely extend over such a large area and they must be severe indeed to be detected against the signal of the surrounding unaffected areas. This coarse spatial resolution prevents a general detection of land use change, even using higher temporal resolution of NDVI time series (fortnightly in this case); (2) it is assumed that abrupt land use changes correlate with abrupt changes in NDVI, however abrupt NDVI changes could also have occurred, *e.g.* because of large-scale ecosystem disturbances such as fires, volcanic eruptions and strong El Niño events, which all directly influence the NDVI values *e.g.* by affecting the reflection of red and near-infrared light. These causes might be distinguished step by step and case by case but globally it might appear difficult due to lack of consistent time series data on fires, volcanic eruptions and strong El Niño events.

In addition, other variables can be derived that may perform better than the selected indicators for detection of abrupt NDVI change. For example, by computing the differences between annual NDVI of consecutive years (this will give 25 values from 1981 – 2006) and comparing the minimum difference (most negative value) with the average of all differences which are negative. With a threshold, *e.g.* the minimum exceeds two times the average decline, cells can be detected that experienced a large (more than average) decline during 1981 – 2006 which could indicate land use change, such as deforestation. The value of the threshold may be derived from an analysis of cells with and without known land use change. Applying this approach on the positive differences, land use changes with increasing annual NDVI values like forestation could be detected as well. Cells that have this characteristic of abrupt change (either positive or negative) can be set aside when searching for soil degradation/improvement because a negative or positive trend of annual NDVI in these cells during 1981-2006 could be due to land use changes rather than degradation or improvement (assuming both to be slower processes). Global trends of this new indicator should be checked case by case with known changes in land use as was done in this study.

Acknowledgements

This work is part of the PBL project on the Biodiversity, Ecosystem Services and Development (Biodiversiteit, ecosysteemdiensten en ontwikkelingsvraagstukken). We thank Sebastián Torrella for sharing the land use change data for the Chaco region; Rogier de Jong for abrupt NDVI trend change data; and Maurits van den Berg for the link to the deforestation of DR of Congo. We are grateful to Gerard Heuvelink for advice on spatial statistics.

References

- Adámoli, J., S. Torrella, R. Ginzburg & B. Gómez, 2011. Land use change and land degradation in Argentinean Chaco. UBA Report 2011/12, GESEEA, Buenos Aires.
- Bai, Z.G., J.G. Conijn, P.S. Bindraban & B. Rutgers, 2012. Global changes of remotely sensed greenness and simulated biomass production since 1981; Towards mapping global soil degradation. Wageningen, ISRIC, ISRIC Report, 2012/02.
- Bai, Z.G., S. Torrella, J. Adámoli, P.S. Bindraban, R. Ginzburg & B. Gómez, 2013 (in prep). Land Degradation and Land Use Change in Chaco region, Argentina. ISRIC report 2013/xx.
- Batjes, N.H., 2006. ISRIC-WISE derived soil properties on a 5 by 5 arc-minutes global grid (ver. 1.1). Report 2006/02, ISRIC - World Soil Information, Wageningen.
- Conijn, J.G., E.P. Querner, M.L. Rau, H. Hengsdijk, J.W. Kuhlman, G.W. Meijerink, B. Rutgers & P.S. Bindraban, 2011. Agricultural resource scarcity and distribution: a case study of crop production in Africa. Wageningen: Plant Research International, (Report / Plant Research International 380).
- Conijn, J.G., H. Hengsdijk, B. Rutgers & R.E.E. Jongschaap, 2011a. Mapping maize yield variability in Mali. Wageningen: Plant Research International, Report / Plant Research International 375.
- CRU [University of East Anglia Climatic Research Unit], 2011. CRU Time Series (TS) high resolution gridded datasets, [Internet]. NCAS British Atmospheric Data Centre. Available from http://badc.nerc.ac.uk/view/badc.nerc.ac.uk_ATOM_dataent_1256223773328276 Accessed November 15, 2011.
- Erb, K.H., V. Gaube, F. Krausmann, C. Plutzer, A. Bondeau & H. Haberl, 2007. A comprehensive global 5 min resolution land-use dataset for the year 2000 consistent with national census data. *Journal of land use science*, 2, 191–224.
- FAO [Food and Agriculture Organization], 1996. Digital soil map of the world and derived soil properties, version 3.5, November 1995, derived from the FAO/UNESCO soil map of the world, original scale 1:5 000 000. CDRom, FAO, Rome.
- Fensholt, R., I. Sandholt & M.S. Rasmussen, 2004. Evaluation of MODIS LAI, fAPAR and the relation between fAPAR and NDVI in a semi-arid environment using in situ measurements. *Remote Sensing of Environment*, 91, 490-507.
- Fensholt, R., Sandholt, I., Rasmussen, M.S., Stison, S. & Diouf, A., 2006. Evaluation of satellite-based primary production modelling in the semi-arid Sahel. *Remote Sensing of the Environment*, 105 173-188.
- Gebremichael, M. & Barros, A.P., 2006. Evaluation of MODIS gross primary productivity (GPP) in tropical monsoon regions. *Remote Sensing of Environment*, 100, 150-166.
- Heinsch, F.A., M. Reeves, P. Votava & others, 2003. User's Guide: GPP and NPP (MOD17A2/A3) Products NASA MODIS Land Algorithm Version 20, December 2, 2003. University of Montana.
- Holben, B.N., 1986. Characteristics of maximum-value composite images from temporal AVHRR data. *International Journal of Remote Sensing*, 7, 1417-1434.
- Jing, Q., J.G. Conijn, R.E.E. Jongschaap & P.S. Bindraban, 2012. Modeling the productivity of energy crops in different agro-ecological environments. Biomass and Bioenergy, available online 27 July 2012 (<http://www.sciencedirect.com/science/article/pii/S0961953412002772>)

- Jong, R. de, J. Verbesselt, M.E. Schaepman & S. de Bruin, 2012. Trend changes in global greening and browning: contribution of short-term trends to longer-term change. *Global Change Biology*, 18, 642–655, doi: 10.1111/j.1365-2486.2011.02578.x.
- JRC, 2006. *Global Land Cover 2000 database*. European Commission, Joint Research Centre, <http://www.gem.jrc.it/glc2000>.
- Kaufmann, R.K., L. Zhou, Y. Knyazikhin, V. Shabanov, R.B. Myneni & C.J. Tucker, 2000. Effect of orbital drift and sensor changes on the time series of AVHRR vegetation index data. *IEEE Transactions on Geoscience and Remote Sensing*, 38, 2584-2597.
- Nagol, J.R., E.F. Vermote & S.D. Prince, 2009. Effects of atmospheric variation on AVHRR NDVI data. *Remote Sensing of Environment*, 113, 392-397.
- Nemani, R.R., C.D. Keeling, H. Hashimoto & others, 2003. Climate-driven increases in global terrestrial net primary production from 1982 to 1999. *Science*, 300, 1560-1563.
- OSFAC, 2010. Atlas of forest cover and change 2000–2010 in the Democratic Republic of the Congo. Prepared by Observatoire satellital des forêts d’Afrique centrale (OSFAC), South Dakota State University (SDSU), University of Maryland (UMD).
- Pinzon, J.E., M.E. Brown & C.J. Tucker, 2007. Global Inventory Modeling and Mapping Studies (GIMMS) satellite-drift corrected and NOAA-16 incorporated Normalized Difference Vegetation Index (NDVI), monthly 1981-2006. University of Maryland Global Land Cover Facility Data Distribution.
- Pinzon, J.E., M.E. Brown & C.J. Tucker. Satellite time series correction of orbital drift artifacts using empirical mode decomposition N. Huang (Ed.), Hilbert-Huang Transform: Introduction and Applications (2005), pp. 167–186.
- Roerink, G.J., M. Menenti & W. Verhoef, 2000. Reconstructing cloud free NDVI composites using Fourier analysis of time series. *International Journal of Remote Sensing*, 21, 1911–1917.
- Running, S.W., F.A. Heinsch, M. Zhao, M. Reeves & H. Hashimoto, 2004. A continuous satellite-derived measure of global terrestrial production. *Bioscience*, 54, 547-560.
- Sukhinin, A.I., N.H.F. French, E.S. Kasischke, J.H. Hewson, A.J. Soja, I.A. Csiszar, E.J. Hyer, T. Loboda, S.G. Conrad, V.I. Romasko, E.A. Pavlichenko, S.I. Miskiv & O.A. Slinkina, 2004. AVHRR-based mapping of fires in Russia: New products for fire management and carbon cycle studies. *Remote Sensing of Environment*, 93, 546–564.
- Tucker, C.J., J. Pinzon, M.E. Brown, D.S. Slayback, E.W. Pak, R. Mahoney, E. Vermote & N.E. Saleous, 2005. An extended AVHRR 8 km NDVI dataset compatible with MODIS and SPOT vegetation NDVI data. *International Journal of Remote Sensing*, 26, 4485–4498.
- Tucker, C.J., J.E. Pinzon & M.E. Brown, 2004. Global Inventory Modeling and Mapping Studies (GIMMS) satellite drift corrected and NOAA-16 incorporated normalised difference vegetation index (NDVI), monthly 1981–2002. University of Maryland.
- Turner, D.P., W.D. Ritts, W.B. Cohen, S.T. Gower, S.W. Running, M. Zhao, M.H. Costa, A. Kirschbaum, J. Ham, S. Saleska & D.E. Ahl, 2006. Evaluation of MODIS NPP and GPP products across multiple biomes. *Remote Sensing of Environment*, 102:282–292.
- Turner, D.P., W.D. Ritts, W.B. Cohen, S.T. Gower, M.S. Zhao, S.W. Running, S.C. Wofsy, S. Urbanski, A.L. Dunn & J.W. Munger, 2003. *Scaling Gross Primary Production (GPP) over boreal and deciduous forest landscapes in support of MODIS GPP product validation*. *Remote Sensing of Environment*, 88, 256–270.
- Verhoef, W., M. Menenti & S. Azzali, 1996. A colour composite of NOAA-AVHRR-NDVI based on time series analysis (1981-1992). *International Journal of Remote Sensing*, 17, 231–235.

- Wit, A.J.W. de & B. Su, 2005. Deriving phenological indicators from SPOT-VGT data using the HANTS algorithm. In, *2nd international SPOT-VEGETATION user conference* (pp. 195-201). Antwerp, Belgium.
- Zhao, M. & S.W. Running, 2010. Drought-induced reduction in global terrestrial net primary production from 2000 through 2009. *Science*, 329, 940–943.
- Zhao, M., F.A. Heinsch, R.R. Nemani & S.W. Running, 2005. Improvements of the MODIS terrestrial gross and net primary production global data set. *Remote Sensing of Environment*, 95, 164–176.

Appendix I Global mapping of abrupt changes

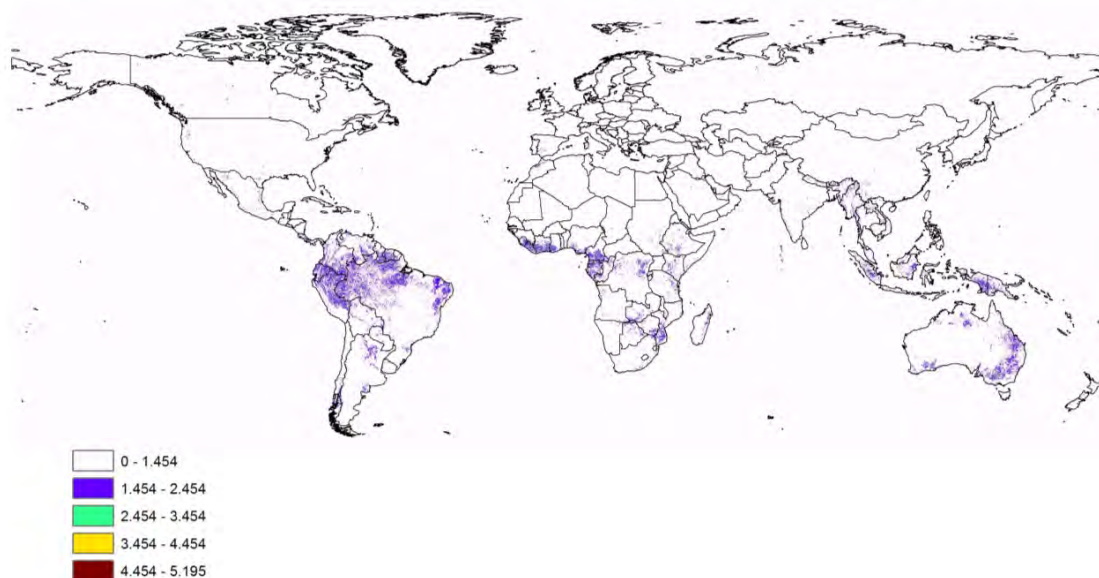


Figure A1

Differences between multi-year mean Σ NDVI and minimum Σ NDVI during 1981–2006

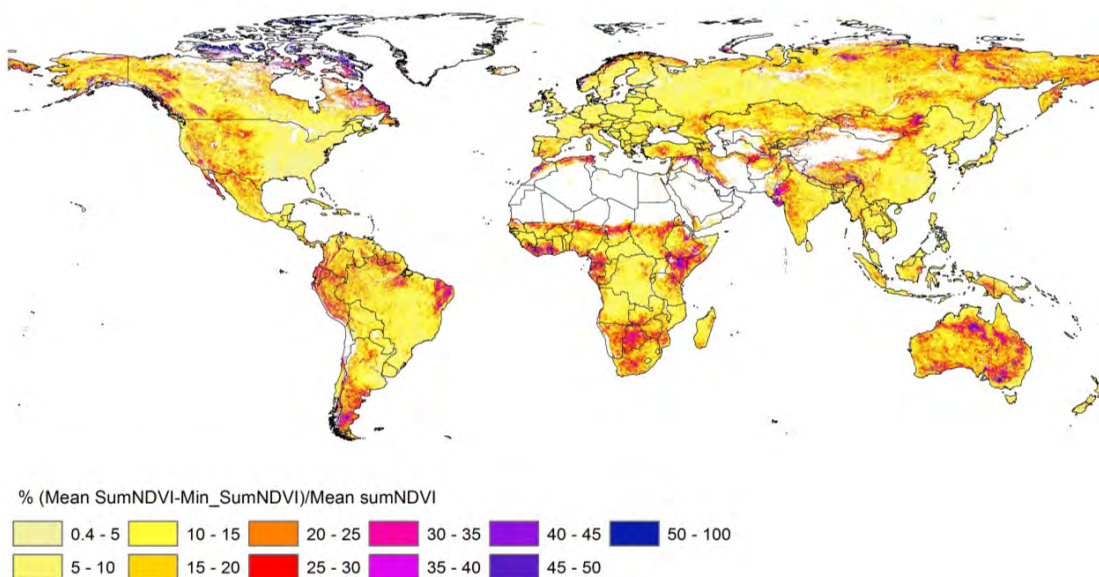


Figure A2

Percentage of (Mean Σ NDVI - Min Σ NDVI) / Mean Σ NDVI from 1981–2006.

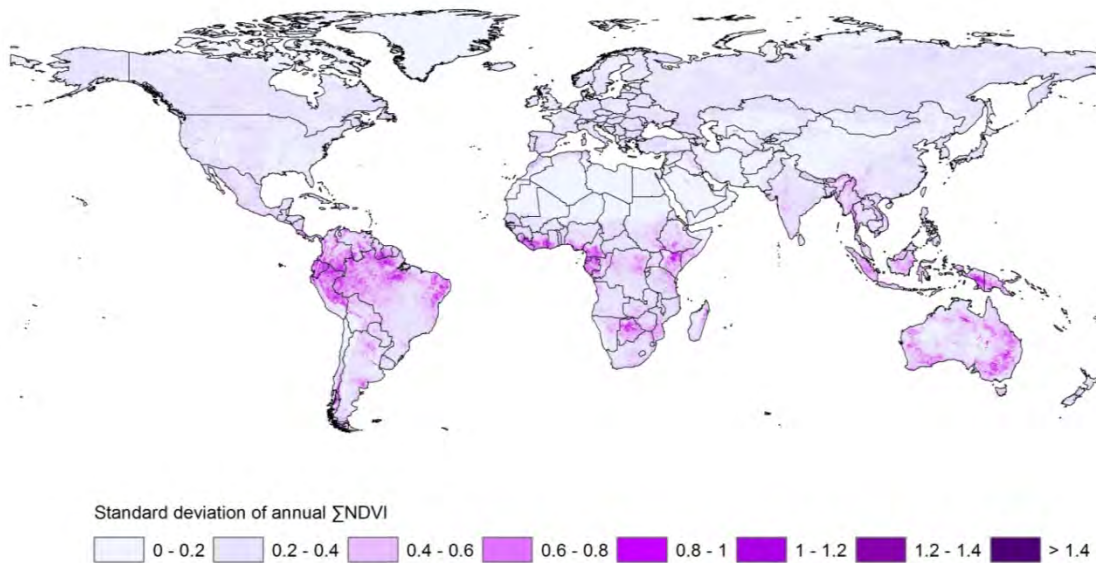


Figure A3
Standard deviation of annual Σ NDVI from 1981–2006.



ISRIC – World Soil Information has a mandate to serve the international community as custodian of global soil information and to increase awareness and understanding of soils in major global issues.

More information: www.isric.org